4

SCATTERING FROM RANDOMLY PERTURBED PERIODIC AND QUASIPERIODIC SURFACES

H. A. Yueh, R. T. Shin, and J. A. Kong

4.1 Introduction

Scattering of electromagnetic waves from a randomly perturbed periodic surface is of interest in the active remote sensing of plowed field and ocean surface. The variations of the radar scattering coefficients due to the change in the look direction relative to the row direc-

tion have been well documented [Batlivala and Ulaby, 1976; Ulaby and Bare, 1979; Fenner *et al.*, 1980]. In the past, the problem of electromagnetic wave scattering from periodic [Waterman, 1975; Jordan and Lang, 1979; Chuang and Kong, 1982] or random [Rice, 1951; Beckmann and Spizzichino, 1963; Stogryn, 1967; Valenzuela, 1967; Sancer, 1969; Leader, 1971; Tsang and Kong, 1980a] rough surfaces has been extensively studied. The problem of scattering by randomly perturbed surface has been studied by assuming that the periodic surface causes a tilting effect [Ulaby *et al.*, 1982]. In this approach the scattering coefficients of the random rough surfaces obtained using the Kirchhoff approximation or small perturbation method is averaged over the change in local incidence angle due to the periodic surface. This approach has also been used to solve the scattering from a composite random rough surface with small and large variations [Semenov, 1966; Wu and Fung, 1972].

In section 4.2, we use the Extended Boundary Condition (EBC) method to formulate the scattering of electromagnetic waves from a randomly perturbed dielectric periodic surface, and apply the small perturbation method (SPM) to solve the surface currents and scattered fields. The surface currents and the scattered fields are expanded and solved up to the second order. The zeroth order problem which is the scattering from periodic surface is solved exactly. This solution is then used in the small perturbation method to solve for the higher order scattered field from a randomly perturbed periodic surface. The random perturbation is modeled as a Gaussian random process. The theoretical results are illustrated by calculating the bistatic and backscattering coefficients and comparing these with the results obtained using the Kirchhoff approximation.

In section 4.3, we use the Kirchhoff approximation to study the scattering of electromagnetic waves from a randomly perturbed quasi-periodic surface in order to more realistically model the plowed fields. In the plowed fields there are some random variations on the period and amplitude of the sinusoidal variation as we move from one row to the next. This variation can be modelled by introducing the narrow-band Gaussian random process on top of the basic sinusoidal variation, which will cause the surface to be quasiperiodic. Therefore, we characterize the rough surface as a composite surface with a Gaussian random variation, a sinusoidal variation and a narrow-band Gaussian random variation around the same spatial frequency. The physical optics inte-

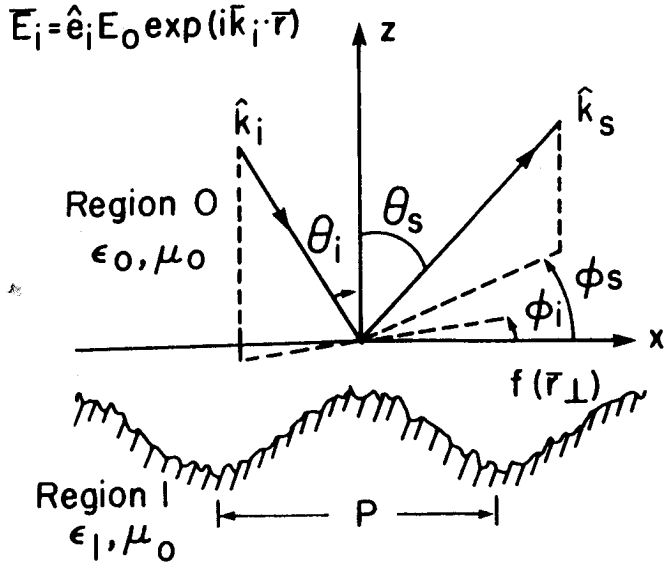

Figure 4.2.1 Geometric configuration of the problem.

gral obtained with the Kirchhoff approximation is evaluated to obtain the coherent and incoherent bistatic scattering coefficients. In the geometrical optics limit, the stationary phase method is used to further simplify the results. In this limit it can be shown that the bistatic scattering coefficients are proportional to the probability of the occurrence of the slopes which will specularly reflect the incident wave into the observation direction. The theoretical results are illustrated for the various cases by plotting the backscattering cross sections as a function of the angle of incidence with the incident wave vector either parallel or perpendicular to the row direction. The appearances of peaks will be explained in terms of the scattering patterns for sinusoidal surfaces.

4.2 Scattering by a Randomly Perturbed Periodic Surface

a. Formulation

Consider a plane wave incident upon a periodic surface with rough-

ness (Fig. 4.2.1). The electric field of the incident wave is given by

$$\overline{E}_i = \hat{e}_i E_0 \exp(i\overline{k}_i \cdot \overline{r}) \tag{1}$$

where

$$\overline{k}_i = \overline{k}_{\perp i} + \hat{z}k_{zi} = \hat{x}k_{xi} + \hat{y}k_{yi} + \hat{z}k_{zi} \tag{2}$$

denotes the incident wave vector, and $\hat{e}_i$ is the unit vector in the polarization direction of the incident electric field. The rough surface is characterized by a height function $z = f(x,y)$, which is given by

$$f(x,y) = H\cos(\frac{2\pi}{p}x) + \xi(x,y) \tag{3}$$

where $\xi(x,y)$ is a small random perturbation on the top of a sinusoidal surface and is modelled as a Gaussian random process with zero mean,

$$< \xi(x,y) >= 0 \tag{4}$$

From Huygens' principle the electric field $\overline{E}(\overline{r})$ in the free space and the transmitted field $\overline{E}_1(\overline{r})$ in the dielectric medium satisfy the following equations [Tsang et al., 1985; Kong, 1986]:

$$\overline{E}_i(\overline{r}) + \int_{S'} dS' \left\{ i\omega\mu_0 \overline{\overline{G}}(\overline{r},\overline{r}') \cdot [\hat{n} \times \overline{H}(\overline{r}')] + \nabla \times \overline{\overline{G}}(\overline{r},\overline{r}') \cdot [\hat{n} \times \overline{E}(\overline{r}')] \right\}$$

$$= \begin{cases} \overline{E}(\overline{r}) & z > f(\overline{r}_\perp) \quad (5a) \\ 0 & z < f(\overline{r}_\perp) \quad (5b) \end{cases}$$

$$- \int_{S'} dS' \left\{ i\omega\mu_1 \overline{\overline{G}}_1(\overline{r},\overline{r}') \cdot [\hat{n} \times \overline{H}_1(\overline{r}')] + \nabla \times \overline{\overline{G}}_1(\overline{r},\overline{r}') \cdot [\hat{n} \times \overline{E}_1] \right\}$$

$$= \begin{cases} 0 & z > f(\overline{r}_\perp) \quad (6a) \\ \overline{E}_1(\overline{r}) & z < f(\overline{r}_\perp) \quad (6b) \end{cases}$$

where $\overline{\overline{G}}(\overline{r},\overline{r}')$ and $\overline{\overline{G}}_1(\overline{r},\overline{r}')$ are the dyadic Green's functions for free space and the homogeneous dielectric of region 1 [Tsang et al., 1985], respectively, and the surface integration is to be carried out over the rough surface S'. The unit vector normal to the rough surface $\hat{n}$ points into the free space

$$\hat{n} = \frac{-\alpha\hat{x} - \beta\hat{y} + \hat{z}}{\sqrt{1 + \alpha^2 + \beta^2}} \tag{7}$$

where α and β are the local slopes in the x and y directions,

$$\alpha = \frac{\partial f(x', y')}{\partial x'} \tag{8a}$$

$$\beta = \frac{\partial f(x', y')}{\partial y'} \tag{8b}$$

Since tangential fields are continuous, we can define surface field unknowns as

$$dS' \sqrt{\frac{\mu_o}{\epsilon_o}} \hat{n} \times \overline{H}(\overline{r}') = d\overline{r}'_\perp \overline{a}(\overline{r}'_\perp) = dS' \sqrt{\frac{\mu_o}{\epsilon_o}} \hat{n} \times \overline{H}_1(\overline{r}') \tag{9a}$$

$$dS' \hat{n} \times \overline{E}(\overline{r}') = d\overline{r}'_\perp \overline{b}(\overline{r}'_\perp) = dS' \hat{n} \times \overline{E}_1(\overline{r}') \tag{9b}$$

where $d\overline{r}'_\perp$ is the projection of dS' on the x-y plane, and the surface fields are tangential to the surface. Thus

$$\hat{n}(\overline{r}'_\perp) \cdot \overline{a}(\overline{r}'_\perp) = 0 \tag{10a}$$

$$\hat{n}(\overline{r}'_\perp) \cdot \overline{b}(\overline{r}'_\perp) = 0 \tag{10b}$$

Let f_{min} and f_{max} be, respectively, the minimum and maximum values of the surface profiles $f(\overline{r})$. Evaluating (5b) for $z < f_{min}$ and (6a) for $z > f_{max}$, we obtain

$$\begin{aligned} \overline{E}_i(\overline{r}) = & \frac{1}{8\pi^2} \int d\overline{k}_\perp e^{i\overline{k}_\perp \cdot \overline{r}_\perp} e^{-ik_z z} \frac{k}{k_z} \int d\overline{r}'_\perp e^{-i\overline{k}_\perp \cdot \overline{r}'_\perp} e^{ik_z f(\overline{r}'_\perp)} \\ & \times \Big\{ [\hat{h}(-k_z)\hat{h}(-k_z) + \hat{v}(-k_z)\hat{v}(-k_z)] \cdot \overline{a}(\overline{r}'_\perp) \\ & + [-\hat{v}(-k_z)\hat{h}(-k_z) + \hat{h}(-k_z)\hat{v}(-k_z)] \cdot \overline{b}(\overline{r}'_\perp) \Big\} \end{aligned} \tag{11a}$$

$$\begin{aligned} 0 = & \frac{1}{8\pi^2} \int d\overline{k}_\perp e^{i\overline{k}_\perp \cdot \overline{r}_\perp} e^{ik_{1z} z} \frac{k_1}{k_{1z}} \int d\overline{r}'_\perp e^{-i\overline{k}_\perp \cdot \overline{r}'_\perp} e^{-ik_{1z} f(\overline{r}'_\perp)} \\ & \times \Big\{ \frac{k}{k_1} [\hat{h}_1(k_{1z})\hat{h}_1(k_{1z}) + \hat{v}_1(k_{1z})\hat{v}_1(k_{1z})] \cdot \overline{a}(\overline{r}'_\perp) \\ & + [-\hat{v}_1(k_{1z})\hat{h}_1(k_{1z}) + \hat{h}_1(k_{1z})\hat{v}_1(k_{1z})] \cdot \overline{b}(\overline{r}'_\perp) \Big\} \end{aligned} \tag{11b}$$

where

$$\bar{k} = \bar{k}_\perp + \hat{z}k_z = \hat{x}k_x + \hat{y}k_y + \hat{z}k_z, \quad k = \omega\sqrt{\mu_o\epsilon_o} \tag{12a}$$

$$\bar{k}_1 = \bar{k}_\perp + \hat{z}k_{1z} = \hat{x}k_x + \hat{y}k_y + \hat{z}k_{1z}, \quad k_1 = \omega\sqrt{\mu_o\epsilon_1} \tag{12b}$$

$$k_\rho = \sqrt{k_x^2 + k_y^2}, \quad k_z = \sqrt{k^2 - k_\rho^2}, \quad k_{1z} = \sqrt{k_1^2 - k_\rho^2} \tag{12c}$$

$$\hat{h}(k_z) = \frac{\hat{k} \times \hat{z}}{|\hat{k} \times \hat{z}|} = \frac{1}{k_\rho}(\hat{x}k_y - \hat{y}k_x) \tag{12d}$$

$$\hat{v}(k_z) = \frac{1}{k}\hat{h} \times \bar{k} = \frac{-k_z}{kk_\rho}(\hat{x}k_x + \hat{y}k_y) + \frac{k_\rho}{k}\hat{z} \tag{12e}$$

$$\hat{h}_1(k_{1z}) = \frac{\hat{k}_1 \times \hat{z}}{|\hat{k}_1 \times \hat{z}|} = \frac{1}{k_\rho}(\hat{x}k_y - \hat{y}k_x) \tag{12f}$$

$$\hat{v}_1(k_{1z}) = \frac{1}{k_1}\hat{h}_1 \times \bar{k}_1 = \frac{-k_{1z}}{k_1k_\rho}(\hat{x}k_x + \hat{y}k_y) + \frac{k_\rho}{k_1}\hat{z} \tag{12g}$$

The above equations are the Extended Boundary Conditions, and are used to solve for the surface fields along with (10). Using (7), (10) can be written as

$$a_z(\bar{r}'_\perp) = (\hat{x}\frac{\partial f(\bar{r}'_\perp)}{\partial x'} + \hat{y}\frac{\partial f(\bar{r}'_\perp)}{\partial y'}) \cdot \bar{a}_\perp(\bar{r}'_\perp) \tag{13a}$$

$$b_z(\bar{r}'_\perp) = (\hat{x}\frac{\partial f(\bar{r}'_\perp)}{\partial x'} + \hat{y}\frac{\partial f(\bar{r}'_\perp)}{\partial y'}) \cdot \bar{b}_\perp(\bar{r}'_\perp) \tag{13b}$$

where a_z and b_z are the z components of $\bar{a}$ and $\bar{b}$, respectively.

Once the surface fields are obtained, then the scattered field $\bar{E}_s(\bar{r})$ in region 0 can be derived by evaluating (5a) for $z > f_{max}$. Thus, we obtain

$$\begin{aligned}\bar{E}_s(\bar{r}) = -\frac{1}{8\pi^2}\int d\bar{k}_\perp e^{i\bar{k}_\perp \cdot \bar{r}_\perp} e^{ik_z z}\frac{k}{k_z}\int d\bar{r}'_\perp e^{-i\bar{k}_\perp \cdot \bar{r}'_\perp} e^{-ik_z f(\bar{r}'_\perp)} \\ \times \Big\{ [\hat{h}(k_z)\hat{h}(k_z) + \hat{v}(k_z)\hat{v}(k_z)] \cdot \bar{a}(\bar{r}'_\perp) \\ + [-\hat{v}(k_z)\hat{h}(k_z) + \hat{h}(k_z)\hat{v}(k_z)] \cdot \bar{b}(\bar{r}'_\perp) \Big\}\end{aligned} \tag{14}$$

Equations (11), (13) and (14) are exact, and the approach is to solve for the surface fields using (11) and (13) and then to solve for the scattered fields using (14).

To solve for the surface fields by perturbation method, let

$$\bar{a}(\bar{r}'_\perp) = \sum_{m=0}^{\infty} \frac{\bar{a}^{(m)}(\bar{r}'_\perp)}{m!} \tag{15a}$$

$$\bar{b}(\bar{r}'_\perp) = \sum_{m=0}^{\infty} \frac{\bar{b}^{(m)}(\bar{r}'_\perp)}{m!} \tag{15b}$$

where $\bar{a}^{(m)}$ and $\bar{b}^{(m)}$ are the mth order terms of $\bar{a}$ and $\bar{b}$, respectively. We also have

$$\exp[\pm ik_z f(\bar{r}'_\perp)] = \exp\left[\pm ik_z H \cos(\frac{2\pi x}{p})\right] \sum_{m=0}^{\infty} \frac{[\pm ik_z \xi(\bar{r}'_\perp)]^m}{m!} \tag{16a}$$

$$\exp[\pm ik_{1z} f(\bar{r}'_\perp)] = \exp\left[\pm ik_{1z} H \cos(\frac{2\pi x}{p})\right] \sum_{m=0}^{\infty} \frac{[\pm ik_{1z} \xi(\bar{r}'_\perp)]^m}{m!} \tag{16b}$$

In the small perturbation method (SPM), ξ and its derivatives are regarded as small parameters. Thus we assume

$$k_z \xi(\bar{r}'_\perp),\ k_{1z} \xi(\bar{r}'_\perp),\ \frac{\partial \xi}{\partial x'},\ \frac{\partial \xi}{\partial y'} \ll 1 \tag{17}$$

Substituting (15) into (13) and equating the same order terms, we have

$$a_z^{(0)}(\bar{r}'_\perp) = \frac{-2\pi H}{P} \sin\left(\frac{2\pi}{P} x\right) a_x^{(0)} \tag{18a}$$

$$b_z^{(0)}(\bar{r}'_\perp) = \frac{-2\pi H}{P} \sin\left(\frac{2\pi}{P} x\right) b_x^{(0)} \tag{18b}$$

$$a_z^{(m)}(\bar{r}'_\perp) = \frac{-2\pi H}{P} \sin\left(\frac{2\pi}{P} x\right) a_x^{(m)} + m\left(\hat{x} \frac{\partial \xi(\bar{r}'_\perp)}{\partial x'} + \hat{y} \frac{\partial \xi(\bar{r}'_\perp)}{\partial y'}\right) \cdot \bar{a}_\perp^{(m-1)}(\bar{r}'_\perp) \tag{18c}$$

$$b_z^{(m)}(\bar{r}'_\perp) = \frac{-2\pi H}{P} \sin\left(\frac{2\pi}{P} x\right) b_x^{(m)} + m\left(\hat{x} \frac{\partial \xi(\bar{r}'_\perp)}{\partial x'} + \hat{y} \frac{\partial \xi(\bar{r}'_\perp)}{\partial y'}\right) \cdot \bar{b}_\perp^{(m-1)}(\bar{r}'_\perp) \tag{18d}$$

Similarly, substituting (15) and (16) into (11) and equating the same order terms, we can calculate the surface fields to different orders. Then, from (14), the scattered fields can be calculated to each order. In the following, we solve for the surface fields and scattered fields up to the second-order. The zeroth-order solutions are just the Bragg diffracted fields from a periodic surface. The first-order solution gives the lowest order incoherent scattered intensities. When the incident direction is perpendicular to the row direction of the periodic surface, the first-order solution does not give the depolarization effect in the backscattering direction. The second-order solution gives the depolarized scattered fields even when the incident direction is perpendicular to the row direction and also the lowest order correction to the coherent fields.

Zeroth-order solution

Substituting only the lowest order terms in the expansion of (15) and (16) into (11), the zeroth-order equations are given by

$$\overline{E}_i(\bar{r}) = \frac{1}{8\pi^2}\int d\bar{k}_\perp e^{i\bar{k}_\perp\cdot\bar{r}_\perp}e^{-ik_{zz}}\frac{k}{k_z}\int d\bar{r}'_\perp e^{-i\bar{k}_\perp\cdot\bar{r}'_\perp}\exp\left[ik_zH\cos(\frac{2\pi x'}{p})\right]$$
$$\times\left\{[\hat{h}(-k_z)\hat{h}(-k_z)+\hat{v}(-k_z)\hat{v}(-k_z)]\cdot\bar{a}^{(0)}(\bar{r}'_\perp)\right.$$
$$\left.+[-\hat{v}(-k_z)\hat{h}(-k_z)+\hat{h}(-k_z)\hat{v}(-k_z)]\cdot\bar{b}^{(0)}(\bar{r}'_\perp)\right\} \tag{19a}$$

$$0 = \frac{1}{8\pi^2}\int d\bar{k}_\perp e^{i\bar{k}_\perp\cdot\bar{r}_\perp}e^{ik_{1z}z}\frac{k_1}{k_{1z}}\int d\bar{r}'_\perp e^{-i\bar{k}_\perp\cdot\bar{r}'_\perp}\exp\left[-ik_{1z}H\cos(\frac{2\pi x'}{p})\right]$$
$$\times\left\{\frac{k}{k_1}[\hat{h}_1(k_{1z})\hat{h}_1(k_{1z})+\hat{v}_1(k_{1z})\hat{v}_1(k_{1z})]\cdot\bar{a}^{(0)}(\bar{r}'_\perp)\right.$$
$$\left.+[-\hat{v}_1(k_{1z})\hat{h}_1(k_{1z})+\hat{h}_1(k_{1z})\hat{v}_1(k_{1z})]\cdot\bar{b}^{(0)}(\bar{r}'_\perp)\right\} \tag{19b}$$

To solve the above equations, the incident electric field is written as

$$\overline{E}_i(\bar{r}) = \hat{e}_iE_oe^{i\bar{k}_{\perp i}\cdot\bar{r}_\perp-ik_{zi}z}$$
$$= \frac{\hat{e}_i}{4\pi^2}\int d\bar{k}_\perp e^{i\bar{k}_\perp\cdot\bar{r}_\perp-ik_{zz}}\int d\bar{r}'_\perp e^{i\bar{k}_{\perp i}\cdot\bar{r}'_\perp-i\bar{k}_\perp\cdot\bar{r}'_\perp} \tag{20}$$

Since the zeroth-order solutions are exactly the scattered fields from a periodic surface, the zeroth-order surface currents can then be expanded by the Floquet modes [Chuang and Kong, 1981 and 1982]. Let

$$a_x^{(0)} = \sum_{n=-\infty}^{\infty} \alpha_{xn}^{(0)} e^{i\bar{k}_{\perp i}\cdot\bar{r}_\perp} e^{i\frac{2n\pi}{p}x} \tag{21a}$$

$$a_y^{(0)} = \sum_{n=-\infty}^{\infty} \alpha_{yn}^{(0)} e^{i\bar{k}_{\perp i}\cdot\bar{r}_\perp} e^{i\frac{2n\pi}{p}x} \tag{21b}$$

$$b_x^{(0)} = \sum_{n=-\infty}^{\infty} \beta_{xn}^{(0)} e^{i\bar{k}_{\perp i}\cdot\bar{r}_\perp} e^{i\frac{2n\pi}{p}x} \tag{21c}$$

$$b_y^{(0)} = \sum_{n=-\infty}^{\infty} \beta_{yn}^{(0)} e^{i\bar{k}_{\perp i}\cdot\bar{r}_\perp} e^{i\frac{2n\pi}{p}x} \tag{21d}$$

where $\bar{r}_\perp = x\hat{x} + y\hat{y}$, and $a_x^{(0)}$, $a_y^{(0)}$, $b_x^{(0)}$, and $b_y^{(0)}$ are the corresponding x and y components of $\bar{a}^{(0)}$ and $\bar{b}^{(0)}$. Substituting (20) and (21) into (19), we have the following matrix equation:

$$M^{(0)} \begin{bmatrix} \alpha_x^{(0)} \\ \alpha_y^{(0)} \\ \beta_x^{(0)} \\ \beta_y^{(0)} \end{bmatrix} = \begin{bmatrix} \hat{h}(-k_{zi})\cdot\hat{e}_i\delta_m \\ \hat{v}(-k_{zi})\cdot\hat{e}_i\delta_m \\ 0 \\ 0 \end{bmatrix} \tag{22}$$

where $\alpha_x^{(0)}$, $\alpha_y^{(0)}$, $\beta_x^{(0)}$ and $\beta_y^{(0)}$ are the column vectors of $\alpha_{xn}^{(0)}$, $\alpha_{yn}^{(0)}$, $\beta_{xn}^{(0)}$ and $\beta_{yn}^{(0)}$, respectively. The matrix equation (22) is given explicitly in Appendix A.

Once (22) is solved, the zeroth-order scattered field $\bar{E}_s^{(0)}(\bar{r})$ is given by

$$\bar{E}_s^{(0)}(\bar{r}) = \sum_{m=-\infty}^{\infty} e^{i\bar{k}_{\perp mi}\cdot\bar{r}_\perp} e^{ik_{zmi}z} [\hat{h}(k_{zmi}) E_{hsm}^{(0)} + \hat{v}(k_{zmi}) E_{vsm}^{(0)}] \tag{23a}$$

where

$$\begin{bmatrix} E_{hs}^{(0)} \end{bmatrix} = H_s^{(0)} \begin{bmatrix} \alpha_x^{(0)} \\ \alpha_y^{(0)} \\ \beta_x^{(0)} \\ \beta_y^{(0)} \end{bmatrix} = H_s^{(0)} M^{(0)-1} \begin{bmatrix} \hat{h}(-k_{zi})\cdot\hat{e}_i\delta_m \\ \hat{v}(-k_{zi})\cdot\hat{e}_i\delta_m \\ 0 \\ 0 \end{bmatrix} \tag{23b}$$

$$\begin{bmatrix} E_{vs}^{(0)} \end{bmatrix} = V_s^{(0)} \begin{bmatrix} \alpha_x^{(0)} \\ \alpha_y^{(0)} \\ \beta_x^{(0)} \\ \beta_y^{(0)} \end{bmatrix} = V_s^{(0)} M^{(o)-1} \begin{bmatrix} \hat{h}(-k_{zi}) \cdot \hat{e}_i \delta_m \\ \hat{v}(-k_{zi}) \cdot \hat{e}_i \delta_m \\ 0 \\ 0 \end{bmatrix} \tag{23c}$$

$$\bar{k}_{\perp mi} = \bar{k}_{\perp i} + \hat{x} \frac{2\pi m}{p}, \quad k_{zmi} = \sqrt{k^2 - k_{\perp mi}^2} \tag{23d}$$

and $E_{hs}^{(0)}$ and $E_{vs}^{(0)}$ are the column vectors formed by $E_{hsm}^{(0)}$ and $E_{vsm}^{(0)}$, respectively. The explicit forms of $H_s^{(0)}$, $V_s^{(0)}$, $E_{hsm}^{(0)}$ and $E_{vsm}^{(0)}$ are given in Appendix A.

First-order solution

The first-order equation can be obtained by keeping Eqs. (15) and (16) up to the first order. Substituting the first-order expansion into (11), the following first-order equation can be obtained:

$$\begin{aligned} 0 = \frac{1}{8\pi^2} \int d\bar{k}_\perp e^{i\bar{k}_\perp \cdot \bar{r}_\perp} e^{-ik_z z} \frac{k}{k_z} \int d\bar{r}'_\perp e^{-i\bar{k}_\perp \cdot \bar{r}'_\perp} \exp\left[ik_z H \cos\left(\frac{2\pi}{p}x'\right)\right] \\ \times \Big\{ [\hat{h}(-k_z)\hat{h}(-k_z) + \hat{v}(-k_z)\hat{v}(-k_z)] \\ \cdot [\bar{a}^{(1)}(\bar{r}'_\perp) + ik_z \xi(\bar{r}'_\perp)\bar{a}^{(0)}(\bar{r}'_\perp)] \\ + [-\hat{v}(-k_z)\hat{h}(-k_z) + \hat{h}(-k_z)\hat{v}(-k_z)] \\ \cdot [\bar{b}^{(1)}(\bar{r}'_\perp) + ik_z \xi(\bar{r}'_\perp)\bar{b}^{(0)}(\bar{r}'_\perp)] \Big\} \end{aligned} \tag{24a}$$

$$\begin{aligned} 0 = \frac{1}{8\pi^2} \int d\bar{k}_\perp e^{i\bar{k}_\perp \cdot \bar{r}_\perp} e^{ik_{1z} z} \frac{k_1}{k_{1z}} \int d\bar{r}'_\perp e^{-i\bar{k}_\perp \cdot \bar{r}'_\perp} \exp\left[-ik_{1z} H \cos\left(\frac{2\pi}{p}x'\right)\right] \\ \times \Big\{ \frac{k}{k_1} [\hat{h}_1(k_{1z})\hat{h}_1(k_{1z}) + \hat{v}_1(k_{1z})\hat{v}_1(k_{1z})] \\ \cdot [\bar{a}^{(1)}(\bar{r}'_\perp) - ik_{1z} \xi(\bar{r}'_\perp)\bar{a}^{(0)}(\bar{r}'_\perp)] \\ + [-\hat{v}_1(k_{1z})\hat{h}_1(k_{1z}) + \hat{h}_1(k_{1z})\hat{v}_1(k_{1z})] \\ \cdot [\bar{b}^{(1)}(\bar{r}'_\perp) - ik_{1z} \xi(\bar{r}'_\perp)\bar{b}^{(0)}(\bar{r}'_\perp)] \Big\} \end{aligned} \tag{24b}$$

To solve the first-order equations in the spatial frequency domain, we take the Fourier transform of the first-order surface currents $\bar{a}^{(1)}$, $\bar{b}^{(1)}$

and the roughness function $\xi(x,y)$.

$$A_x^{(1)}(\bar{k}_\perp) = \frac{1}{(2\pi)^2}\int d\bar{r}'_\perp a_x^{(1)}(\bar{r}'_\perp)e^{-i\bar{k}_{\perp i}\cdot\bar{r}'_\perp}e^{-i\bar{k}_\perp\cdot\bar{r}'_\perp} \tag{25a}$$

$$A_y^{(1)}(\bar{k}_\perp) = \frac{1}{(2\pi)^2}\int d\bar{r}'_\perp a_y^{(1)}(\bar{r}'_\perp)e^{-i\bar{k}_{\perp i}\cdot\bar{r}'_\perp}e^{-i\bar{k}_\perp\cdot\bar{r}'_\perp} \tag{25b}$$

$$B_x^{(1)}(\bar{k}_\perp) = \frac{1}{(2\pi)^2}\int d\bar{r}'_\perp b_x^{(1)}(\bar{r}'_\perp)e^{-i\bar{k}_{\perp i}\cdot\bar{r}'_\perp}e^{-i\bar{k}_\perp\cdot\bar{r}'_\perp} \tag{25c}$$

$$B_y^{(1)}(\bar{k}_\perp) = \frac{1}{(2\pi)^2}\int d\bar{r}'_\perp b_y^{(1)}(\bar{r}'_\perp)e^{-i\bar{k}_{\perp i}\cdot\bar{r}'_\perp}e^{-i\bar{k}_\perp\cdot\bar{r}'_\perp} \tag{25d}$$

$$F(\bar{k}_\perp) = \frac{1}{(2\pi)^2}\int d\bar{r}'_\perp \xi(\bar{r}'_\perp)e^{-i\bar{k}_\perp\cdot\bar{r}'_\perp} \tag{26}$$

Substituting (18), (25) and (26) into (24), we have the following matrix equation (The matrix equation is given explicitly in Appendix B.):

$$M^{(1)}\begin{bmatrix} A_x^{(1)} \\ A_y^{(1)} \\ B_x^{(1)} \\ B_y^{(1)} \end{bmatrix} = R^{(1)}\left[F(\bar{k}_\perp - \bar{k}_{\perp mi})\right] \tag{27}$$

where $A_x^{(1)}$, $A_y^{(1)}$, $B_x^{(1)}$, and $B_y^{(1)}$ are the column vectors formed by $A_x^{(1)}(\bar{k}_\perp - \bar{k}_{\perp mi})$, $A_y^{(1)}(\bar{k}_\perp - \bar{k}_{\perp mi})$, $B_x^{(1)}(\bar{k}_\perp - \bar{k}_{\perp mi})$ and $B_y^{(1)}(\bar{k}_\perp - \bar{k}_{\perp mi})$, respectively.

The matrix $R^{(1)}$ is dependent on the zeroth-order solution $\alpha_{xn}^{(0)}$, $\alpha_{yn}^{(0)}$, $\beta_{xn}^{(0)}$ and $\beta_{yn}^{(0)}$. Once the zeroth-order solution is solved, the matrix $R^{(1)}$ can be determined. The above matrix equation accounts for the coupling between the first-order surface fields and the roughness function with the set of frequency components

$$\bar{k}_\perp - \bar{k}_{\perp mi} = \bar{k}_\perp - \bar{k}_{\perp i} - \hat{x}\frac{2m\pi}{p} \qquad m = -\infty, ..., \infty \tag{28}$$

The above coupling equations are due to the Bragg scattering mechanism of the large scale periodic surface. Thus, the first-order solution can be solved in terms of the zeroth-order solution and the Fourier components of the small random perturbation.

Keeping (14) to first order, we have the first-order scattered field.

$$\bar{E}_s^{(1)}(\bar{r}) = \int d\bar{k}_\perp e^{i\bar{k}_\perp\cdot\bar{r}_\perp}e^{ik_z z}\left\{\hat{h}(k_z)\sum_m E_{hsm}^{(1)} + \hat{v}(k_z)\sum_m E_{vsm}^{(1)}\right\} \tag{29}$$

where $E_{hsm}^{(1)}$ and $E_{vsm}^{(1)}$ are linearly dependent on the Fourier components $A_x^{(1)}(\bar{k}_\perp - \bar{k}_{\perp mi})$, $A_y^{(1)}(\bar{k}_\perp - \bar{k}_{\perp mi})$, $B_x^{(1)}(\bar{k}_\perp - \bar{k}_{\perp mi})$, $B_y^{(1)}(\bar{k}_\perp - \bar{k}_{\perp mi})$, and $F(\bar{k}_\perp - \bar{k}_{\perp mi})$.

$$\begin{bmatrix} E_{hs}^{(1)} \end{bmatrix} = H_s^{(1)} \begin{bmatrix} A_x^{(1)} \\ A_y^{(1)} \\ B_x^{(1)} \\ B_y^{(1)} \end{bmatrix} + H_f^{(1)} \begin{bmatrix} F(\bar{k}_\perp - \bar{k}_{\perp mi}) \end{bmatrix}$$

$$= \left(H_s^{(1)} M^{(1)-1} R^{(1)} + H_f^{(1)} \right) \begin{bmatrix} F(\bar{k}_\perp - \bar{k}_{\perp mi}) \end{bmatrix} \tag{30a}$$

$$\begin{bmatrix} E_{vs}^{(1)} \end{bmatrix} = V_s^{(1)} \begin{bmatrix} A_x^{(1)} \\ A_y^{(1)} \\ B_x^{(1)} \\ B_y^{(1)} \end{bmatrix} + V_f^{(1)} \begin{bmatrix} F(\bar{k}_\perp - \bar{k}_{\perp mi}) \end{bmatrix}$$

$$= \left(V_s^{(1)} M^{(1)-1} R^{(1)} + V_f^{(1)} \right) \begin{bmatrix} F(\bar{k}_\perp - \bar{k}_{\perp mi}) \end{bmatrix} \tag{30b}$$

where $E_{hs}^{(1)}$ and $E_{vs}^{(1)}$ are the column matrices formed by $E_{hsm}^{(1)}$ and $E_{vsm}^{(1)}$, respectively, and $H_f^{(1)}$ and $V_f^{(1)}$ are diagonal matrices [Appendix B]. Then we can obtain the following equations by summing up all the components of $E_{hs}^{(1)}$ and $E_{vs}^{(1)}$.

$$\sum_m E_{hsm}^{(1)} = \sum_m A_{hsm}^{(1)} F(\bar{k}_\perp - \bar{k}_{\perp mi}) \tag{31a}$$

$$\sum_m E_{vsm}^{(1)} = \sum_m A_{vsm}^{(1)} F(\bar{k}_\perp - \bar{k}_{\perp mi}) \tag{31b}$$

If the roughness is modelled as a Gaussian random process with zero mean (i.e., $< F(\bar{k}_\perp - \bar{k}_{\perp mi}) >= 0$), the ensemble average of the first-order scattered field is zero,

$$< \bar{E}_s^{(1)}(\bar{r}) >= 0 \tag{32}$$

This means that the first-order scattered field is an incoherent field.

Second-order solution

By keeping the expansion of (15) and (16) up to the second order and substituting the second-order expansion into (11), the following second-order equations can be obtained:

$$0 = \frac{1}{8\pi^2}\int d\bar{k}_\perp e^{i\bar{k}_\perp\cdot\bar{r}_\perp} e^{-ik_z z}\frac{k}{k_z}\int d\bar{r}'_\perp e^{-i\bar{k}_\perp\cdot\bar{r}'_\perp}\exp\left[ik_z H\cos(\frac{2\pi}{p}x')\right]$$
$$\times\Bigg\{[\hat{h}(-k_z)\hat{h}(-k_z)+\hat{v}(-k_z)\hat{v}(-k_z)]$$
$$\cdot\left[\frac{1}{2}\bar{a}^{(2)}(\bar{r}'_\perp)+ik_z\xi(\bar{r}'_\perp)\bar{a}^{(1)}(\bar{r}'_\perp)-\frac{1}{2}k_z^2\xi^2\bar{a}^{(0)}(\bar{r}'_\perp)\right]$$
$$+[-\hat{v}(-k_z)\hat{h}(-k_z)+\hat{h}(-k_z)\hat{v}(-k_z)]$$
$$\cdot\left[\frac{1}{2}\bar{b}^{(2)}(\bar{r}'_\perp)+ik_z\xi(\bar{r}'_\perp)\bar{b}^{(1)}(\bar{r}'_\perp)-\frac{1}{2}k_z^2\xi^2\bar{b}^{(0)}(\bar{r}'_\perp)\right]\Bigg\} \tag{33a}$$

$$0 = \frac{1}{8\pi^2}\int d\bar{k}_\perp e^{i\bar{k}_\perp\cdot\bar{r}_\perp} e^{ik_{1z} z}\frac{k_1}{k_{1z}}\int d\bar{r}'_\perp e^{-i\bar{k}_\perp\cdot\bar{r}'_\perp}\exp\left[-ik_{1z}H\cos(\frac{2\pi}{p}x')\right]$$
$$\times\Bigg\{\frac{k}{k_1}[\hat{h}_1(k_{1z})\hat{h}_1(k_{1z})+\hat{v}_1(k_{1z})\hat{v}_1(k_{1z})]$$
$$\cdot\left[\frac{1}{2}\bar{a}^{(2)}(\bar{r}'_\perp)-ik_{1z}\xi(\bar{r}'_\perp)\bar{a}^{(1)}(\bar{r}'_\perp)-\frac{1}{2}k_{1z}^2\xi^2\bar{a}^{(0)}(\bar{r}'_\perp)\right]$$
$$+[-\hat{v}_1(k_{1z})\hat{h}_1(k_{1z})+\hat{h}_1(k_{1z})\hat{v}_1(k_{1z})]$$
$$\cdot\left[\frac{1}{2}\bar{b}^{(2)}(\bar{r}'_\perp)-ik_{1z}\xi(\bar{r}'_\perp)\bar{b}^{(1)}(\bar{r}'_\perp)-\frac{1}{2}k_{1z}^2\xi^2\bar{b}^{(0)}(\bar{r}'_\perp)\right]\Bigg\} \tag{33b}$$

Taking the Fourier transform of the surface currents and the roughness function ξ, we can solve the second-order equations in the spatial frequency domain.

$$A_x^{(2)}(\bar{k}_\perp)=\frac{1}{(2\pi)^2}\int d\bar{r}'_\perp a_x^{(2)}(\bar{r}'_\perp)e^{-i\bar{k}_{\perp i}\cdot\bar{r}'_\perp}e^{-i\bar{k}_\perp\cdot\bar{r}'_\perp} \tag{34a}$$

$$A_y^{(2)}(\bar{k}_\perp)=\frac{1}{(2\pi)^2}\int d\bar{r}'_\perp a_y^{(2)}(\bar{r}'_\perp)e^{-i\bar{k}_{\perp i}\cdot\bar{r}'_\perp}e^{-i\bar{k}_\perp\cdot\bar{r}'_\perp} \tag{34b}$$

$$B_x^{(2)}(\bar{k}_\perp)=\frac{1}{(2\pi)^2}\int d\bar{r}'_\perp b_x^{(2)}(\bar{r}'_\perp)e^{-i\bar{k}_{\perp i}\cdot\bar{r}'_\perp}e^{-i\bar{k}_\perp\cdot\bar{r}'_\perp} \tag{34c}$$

$$B_y^{(2)}(\bar{k}_\perp)=\frac{1}{(2\pi)^2}\int d\bar{r}'_\perp b_y^{(2)}(\bar{r}'_\perp)e^{-i\bar{k}_{\perp i}\cdot\bar{r}'_\perp}e^{-i\bar{k}_\perp\cdot\bar{r}'_\perp} \tag{34d}$$

Substituting (18), (21), (25), (26) and (34) into (33), we have the following matrix equation, which is given explicitly in Appendix C.

$$M^{(2)}\begin{bmatrix} A_x^{(2)} \\ A_y^{(2)} \\ B_x^{(2)} \\ B_y^{(2)} \end{bmatrix} = R_1^{(2)}\begin{bmatrix} F * A_x^{(1)}(\bar{k}_\perp - \bar{k}_{\perp mi}) \\ F * A_y^{(1)}(\bar{k}_\perp - \bar{k}_{\perp mi}) \\ F * B_x^{(1)}(\bar{k}_\perp - \bar{k}_{\perp mi}) \\ F * B_y^{(1)}(\bar{k}_\perp - \bar{k}_{\perp mi}) \end{bmatrix}$$
$$+ R_2^{(2)}\begin{bmatrix} F * F(\bar{k}_\perp - \bar{k}_{\perp mi}) \end{bmatrix}$$
$$+ R_3^{(2)}\begin{bmatrix} (k_x - k_{xmi})F * A_x^{(1)}(\bar{k}_\perp - \bar{k}_{\perp mi}) \\ (k_y - k_{ymi})F * A_y^{(1)}(\bar{k}_\perp - \bar{k}_{\perp mi}) \\ (k_x - k_{xmi})F * B_x^{(1)}(\bar{k}_\perp - \bar{k}_{\perp mi}) \\ (k_y - k_{ymi})F * B_y^{(1)}(\bar{k}_\perp - \bar{k}_{\perp mi}) \end{bmatrix} \tag{35}$$

where $A_x^{(2)}$, $A_y^{(2)}$, $B_x^{(2)}$, and $B_y^{(2)}$ are the column vectors formed by $A_x^{(2)}(\bar{k}_\perp - \bar{k}_{\perp mi})$, $A_y^{(2)}(\bar{k}_\perp - \bar{k}_{\perp mi})$, $B_x^{(2)}(\bar{k}_\perp - \bar{k}_{\perp mi})$ and $B_y^{(2)}(\bar{k}_\perp - \bar{k}_{\perp mi})$, respectively, and '$*$' denotes convolution.

The second-order equation is similar to the first order equation in that only the spatial frequency components with integer times $2\pi/p$ difference are coupled together. The second-order solution can be solved in terms of the zeroth-order solution, the first-order solution, and the Fourier components of the roughness function.

Keeping (14) to second order, we have the following expressions for the second-order scattered field:

$$\bar{E}_s^{(2)}(\bar{r}) = \int d\bar{k}_\perp e^{i\bar{k}_\perp \cdot \bar{r}_\perp} e^{ik_z z}\left\{\hat{h}(k_z)\sum_m E_{hsm}^{(2)} + \hat{v}(k_z)\sum_m E_{vsm}^{(2)}\right\} \tag{36}$$

$$\begin{bmatrix} E_{hs}^{(2)} \end{bmatrix} = H_1^{(2)}\begin{bmatrix} A_x^{(2)}(\bar{k}_\perp - \bar{k}_{\perp mi}) \\ A_y^{(2)}(\bar{k}_\perp - \bar{k}_{\perp mi}) \\ B_x^{(2)}(\bar{k}_\perp - \bar{k}_{\perp mi}) \\ B_y^{(2)}(\bar{k}_\perp - \bar{k}_{\perp mi}) \end{bmatrix}$$
$$+ H_2^{(2)}\begin{bmatrix} F * A_x^{(1)}(\bar{k}_\perp - \bar{k}_{\perp mi}) \\ F * A_y^{(1)}(\bar{k}_\perp - \bar{k}_{\perp mi}) \\ F * B_x^{(1)}(\bar{k}_\perp - \bar{k}_{\perp mi}) \\ F * B_y^{(1)}(\bar{k}_\perp - \bar{k}_{\perp mi}) \end{bmatrix} + H_3^{(2)}\begin{bmatrix} F * F(\bar{k}_\perp - \bar{k}_{\perp mi}) \end{bmatrix}$$

$$+ H_4^{(2)} \begin{bmatrix} (k_x - k_{xmi})F * A_x^{(1)}(\overline{k}_\perp - \overline{k}_{\perp mi}) \\ (k_y - k_{ymi})F * A_y^{(1)}(\overline{k}_\perp - \overline{k}_{\perp mi}) \\ (k_x - k_{xmi})F * B_x^{(1)}(\overline{k}_\perp - \overline{k}_{\perp mi}) \\ (k_y - k_{ymi})F * B_y^{(1)}(\overline{k}_\perp - \overline{k}_{\perp mi}) \end{bmatrix}$$

$$= \left(H_1^{(2)} M^{(2)-1} R_1^{(2)} + H_2^{(2)}\right) \begin{bmatrix} F * A_x^{(1)}(\overline{k}_\perp - \overline{k}_{\perp mi}) \\ F * A_y^{(1)}(\overline{k}_\perp - \overline{k}_{\perp mi}) \\ F * B_x^{(1)}(\overline{k}_\perp - \overline{k}_{\perp mi}) \\ F * B_y^{(1)}(\overline{k}_\perp - \overline{k}_{\perp mi}) \end{bmatrix}$$

$$+ \left(H_1^{(2)} M^{(2)-1} R_2^{(2)} + H_3^{(2)}\right) \begin{bmatrix} F * F(\overline{k}_\perp - \overline{k}_{\perp mi}) \end{bmatrix}$$

$$+ \left(H_1^{(2)} M^{(2)-1} R_3^{(2)} + H_4^{(2)}\right) \begin{bmatrix} (k_x - k_{xmi})F * A_x^{(1)}(\overline{k}_\perp - \overline{k}_{\perp mi}) \\ (k_y - k_{ymi})F * A_y^{(1)}(\overline{k}_\perp - \overline{k}_{\perp mi}) \\ (k_x - k_{xmi})F * B_x^{(1)}(\overline{k}_\perp - \overline{k}_{\perp mi}) \\ (k_y - k_{ymi})F * B_y^{(1)}(\overline{k}_\perp - \overline{k}_{\perp mi}) \end{bmatrix} \tag{37a}$$

$$\begin{bmatrix} E_{vs}^{(2)} \end{bmatrix} = V_1^{(2)} \begin{bmatrix} A_x^{(2)}(\overline{k}_\perp - \overline{k}_{\perp mi}) \\ A_y^{(2)}(\overline{k}_\perp - \overline{k}_{\perp mi}) \\ B_x^{(2)}(\overline{k}_\perp - \overline{k}_{\perp mi}) \\ B_y^{(2)}(\overline{k}_\perp - \overline{k}_{\perp mi}) \end{bmatrix} + V_2^{(2)} \begin{bmatrix} F * A_x^{(1)}(\overline{k}_\perp - \overline{k}_{\perp mi}) \\ F * A_y^{(1)}(\overline{k}_\perp - \overline{k}_{\perp mi}) \\ F * B_x^{(1)}(\overline{k}_\perp - \overline{k}_{\perp mi}) \\ F * B_y^{(1)}(\overline{k}_\perp - \overline{k}_{\perp mi}) \end{bmatrix}$$

$$+ V_3^{(2)} \begin{bmatrix} F * F(\overline{k}_\perp - \overline{k}_{\perp mi}) \end{bmatrix}$$

$$+ V_4^{(2)} \begin{bmatrix} (k_x - k_{xmi})F * A_x^{(1)}(\overline{k}_\perp - \overline{k}_{\perp mi}) \\ (k_y - k_{ymi})F * A_y^{(1)}(\overline{k}_\perp - \overline{k}_{\perp mi}) \\ (k_x - k_{xmi})F * B_x^{(1)}(\overline{k}_\perp - \overline{k}_{\perp mi}) \\ (k_y - k_{ymi})F * B_y^{(1)}(\overline{k}_\perp - \overline{k}_{\perp mi}) \end{bmatrix}$$

$$= \left(V_1^{(2)} M^{(2)-1} R_1^{(2)} + V_2^{(2)}\right) \begin{bmatrix} F * A_x^{(1)}(\overline{k}_\perp - \overline{k}_{\perp mi}) \\ F * A_y^{(1)}(\overline{k}_\perp - \overline{k}_{\perp mi}) \\ F * B_x^{(1)}(\overline{k}_\perp - \overline{k}_{\perp mi}) \\ F * B_y^{(1)}(\overline{k}_\perp - \overline{k}_{\perp mi}) \end{bmatrix}$$

$$+ \left(V_1^{(2)} M^{(2)-1} R_2^{(2)} + V_3^{(2)}\right) \begin{bmatrix} F * F(\overline{k}_\perp - \overline{k}_{\perp mi}) \end{bmatrix}$$

$$+\left(V_1^{(2)}M^{(2)-1}R_3^{(2)}+V_4^{(2)}\right)\begin{bmatrix}(k_x-k_{xmi})F*A_x^{(1)}(\bar{k}_\perp-\bar{k}_{\perp mi})\\(k_y-k_{ymi})F*A_y^{(1)}(\bar{k}_\perp-\bar{k}_{\perp mi})\\(k_x-k_{xmi})F*B_x^{(1)}(\bar{k}_\perp-\bar{k}_{\perp mi})\\(k_y-k_{ymi})F*B_y^{(1)}(\bar{k}_\perp-\bar{k}_{\perp mi})\end{bmatrix} \tag{37b}$$

where $E_{hs}^{(2)}$ and $E_{vs}^{(2)}$ are the column matrices formed by $E_{hsm}^{(2)}$ and $E_{vsm}^{(2)}$, respectively [Appendix C].

Thereafter (27) is solved and substituted into (37), we can express $E_{hs}^{(2)}$ and $E_{vs}^{(2)}$ in terms of a sum of this kind of components, $fF(\bar{k}_\perp-\bar{k}_{\perp mi})*gF(\bar{k}_\perp-\bar{k}_{\perp ni})$, where f and g are deterministic functions of $\bar{k}_\perp$. If the roughness is modeled as a Gaussian random process, then it can be shown that

$$<fF(\bar{k}_\perp-\bar{k}_{\perp mi})*gF(\bar{k}_\perp-\bar{k}_{\perp ni})>=4\pi^2\delta(\bar{k}_\perp-\bar{k}_{\perp mi}+\bar{k}_{\perp ni})\times\int d\bar{k}'_\perp f(\bar{k}'_\perp)g(\bar{k}_\perp-\bar{k}'_\perp)W(\bar{k}'_\perp-\bar{k}_{\perp mi}) \tag{38}$$

where $W(|\bar{k}_\perp-\bar{k}_{\perp mi}|)$ is the spectral density of the random roughness and is the Fourier transform of the correlation function. The spectral density is given by

$$W(\bar{k}_\perp)=\frac{\sigma^2}{(2\pi)^2}\int d\bar{r}_\perp e^{i\bar{k}_\perp\cdot\bar{r}_\perp}C(\bar{r}_\perp) \tag{39}$$

and satisfies the relation

$$\left\langle F(\bar{k}'_\perp)F^*(\bar{k}_\perp)\right\rangle=\delta(\bar{k}'_\perp-\bar{k}_\perp)W(|\bar{k}'_\perp|) \tag{40}$$

Then from (36) and (37) the ensemble average of the second-order scattered field reduces to a set of plane waves which propagate in the directions of zeroth-order scattered fields. This implies that the coherent second-order scattered fields are the correction to the zeroth-order solution in the Bragg diffraction directions of the periodic surface.

b. Bistatic and Backscattering Coefficients

The lowest order incoherent scattering coefficients can be derived from the first-order scattered fields by considering the horizontally and

vertically polarized incidence and calculating the horizontally and vertically polarized scattered fields. The lowest order incoherent Poynting power flow is averaged over one period and given by

$$\begin{aligned}\overline{S}^{(1)} &= \frac{1}{p}\int_0^p Re\{<\overline{E}_s^{(1)} \times \overline{H}_s^{(1)*}>\}dx \\ &= \int d\overline{k}_\perp \frac{\overline{k}}{\omega\mu} \sum_{m=-\infty}^{\infty} W(|\overline{k}_\perp - \overline{k}_{\perp mi}|)(|A_{hsm}^{(1)}|^2 + |A_{vsm}^{(1)}|^2) \end{aligned} \quad (41)$$

For a Gaussian correlation function $C(\overline{r}_\perp)$, the spectral density is given by

$$W(|\overline{k}_\perp - \overline{k}_{\perp mi}|) = \frac{1}{4\pi}\sigma^2 l^2 \exp[-\frac{1}{4}|\overline{k}_\perp - \overline{k}_{\perp mi}|^2 l^2] \quad (42)$$

where σ is the standard deviation of the random roughness, and l is the correlation length for $\xi(\overline{r}_\perp)$ in the transverse plane.

The bistatic scattering coefficients $\gamma_{ba}(\hat{k}_s, \hat{k}_i)$ are defined as the ratio of scattered power of polarization b_s per unit solid angle in direction $\hat{k}_s$ and the intercepted power of polarization a_i with amplitude E_{ao} in direction $\hat{k}_i$ averaged over 4π radians. Thus, we have

$$\gamma_{ba}(\hat{k}_s, \hat{k}_i) = 4\pi \frac{k^2 \cos^2\theta_s \sum_{m=-\infty}^{\infty} |A_{bsm}^{(1)}|^2 W(|\overline{k}_{\perp s} - \overline{k}_{\perp mi}|)}{\cos\theta_i |E_{ao}|^2} \quad a, b = h, v \quad (43)$$

In the backscattering direction, $\hat{k}_s = -\hat{k}_i$, the backscattering cross section per unit area is defined to be

$$\sigma_{ba}(\hat{k}_i) = \cos\theta_i \, \gamma_{ba}(-\hat{k}_i, \hat{k}_i) \quad (44)$$

where

$$\hat{k}_i = \sin\theta_i \cos\phi_i \hat{x} + \sin\theta_i \sin\phi_i \hat{y} - \cos\theta_i \hat{z} \quad (45a)$$

$$\hat{k}_s = \sin\theta_s \cos\phi_s \hat{x} + \sin\theta_s \sin\phi_s \hat{y} + \cos\theta_s \hat{z} \quad (45b)$$

In the next section, the numerical results of bistatic scattering coefficients and backscattering cross sections per unit area are illustrated as functions of incident and scattered directions.

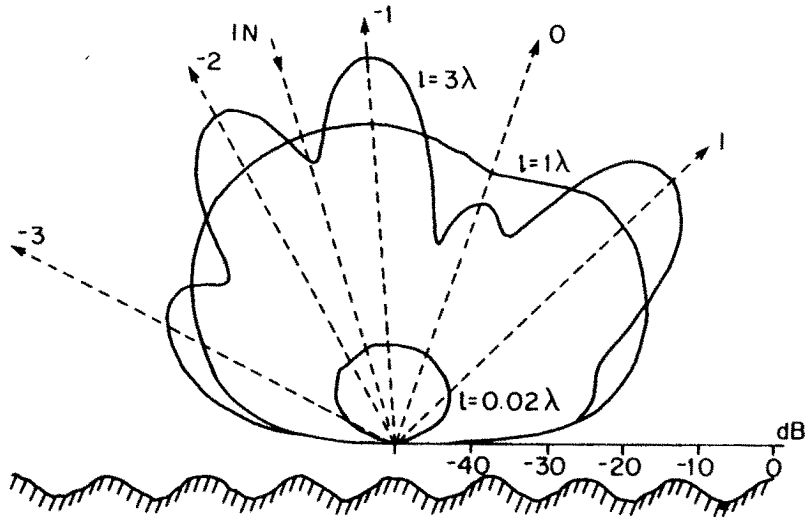

Figure 4.2.2 Scattering pattern γ_{hh} versus θ_s for various correlation lengths $l = 0.02$, 1.0, and 3.0λ with $\theta_i = 18°$, $\phi_i = 0°$, $\sigma = 0.01\lambda$, $H = 100$ nm, $P = 1205$ nm, $\lambda = 482$ nm, and $\epsilon_1 = (-7.29139 + 0.2943871)\epsilon_0$

c. Numerical Results and Discussions

The theoretical results obtained using the EBC/SPM method are illustrated in this section by calculating the bistatic scattering coefficients and the backscattering cross sections per unit area. In Figs. 4.2.2 and 4.2.3 the bistatic scattering coefficients $\gamma_{ba}(\theta_s, \phi_s)$ are plotted in a polar plot versus the scattering angle θ_s for several correlation lengths l. The plane wave is incident perpendicular to the row direction of a sinusoidal silver grating with random roughness. The scattering patterns for horizontally and vertically polarized incident fields are given in Figs. 4.2.2 and 4.2.3, respectively. The electromagnetic wave scattering from this silver grating without roughness has been studied by Chuang and Kong [1981].

In Fig. 4.2.2, the scattering pattern for horizontally polarized incidence is plotted on the incident plane with θ_s varied. When the correlation length is large, there is one peak associated with each Bragg diffraction direction. As the correlation length decreases from $l = 3\lambda$ to $l = 1\lambda$, the beams become broader. This beam shape is determined by (43). The beam width depends on the correlation length and the function $A^{(1)}_{b,m}$. The effect of correlation length on the beam width

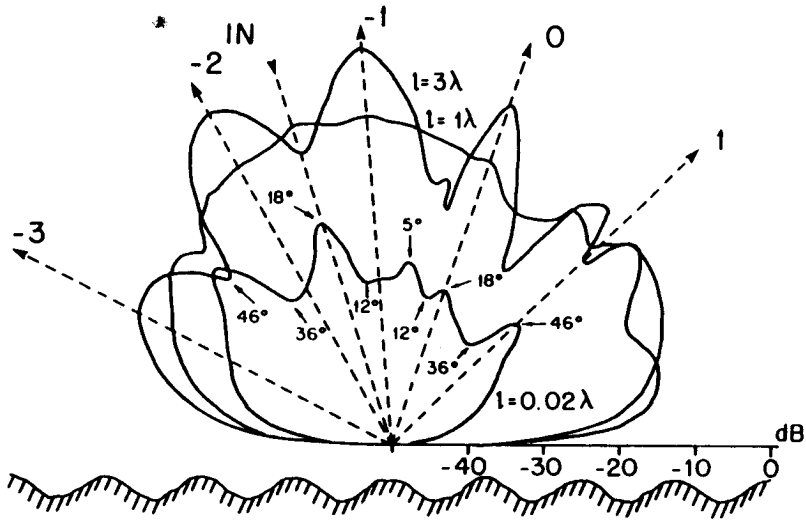

Figure 4.2.3 Scattering pattern γ_{vv} versus θ_s for various correlation lengths $l = 0.02$, 1.0, and 3.0λ with $\theta_i = 18°$, $\phi_i = 0°$, $\sigma = 0.01\lambda$, $H = 100$ nm, $P = 1205$ nm, $\lambda = 482$ nm, and $\epsilon_1 = (-7.29139 + 0.2943871)\epsilon_0$

can be explained as follows. Smaller correlation lengths means that the standard deviation of the slope of the roughness is larger, and the power can be scattered into wider directions. As shown in Fig. 4.2.2, when the correlation length becomes small, say $l = 0.02\lambda$, the power seems to be scattered isotropically into all the directions.

The corresponding scattering pattern for vertically polarized incidence is shown in Fig. 4.2.3. The result is similar to horizontal polarization incidence for large correlation lengths. Again several beams show up for $l = 3\lambda$. However, when the correlation length is $l = 0.02\lambda$, several peaks at $(\theta_s, \phi_s) = (46°, 180°), (18°, 180°), (5°, 0°), (18°, 0°)$, and $(46°, 0°)$ show up in the scattering pattern. As shown in [Chuang and Kong, 1981], the scattered wave is strongly affected by the surface plasmons at $\theta_s = 18°$ and $46°$ which are related to the propagation constants of the guided waves supportable by the periodic surface, and the diffraction efficiencies of mode -1 and -2 show maximum and minimum values, respectively, at $\theta_i = 5°$. If we take a close look at Fig. 4.2.3, we notice that the scattering pattern shows somewhat unsmooth behavior at $(\theta_s, \phi_s) = (12°, 180°), (36°, 180°), (12°, 0°)$ and $(36°, 0°)$. These are related to the Rayleigh wavelength anomalies [Hessel and

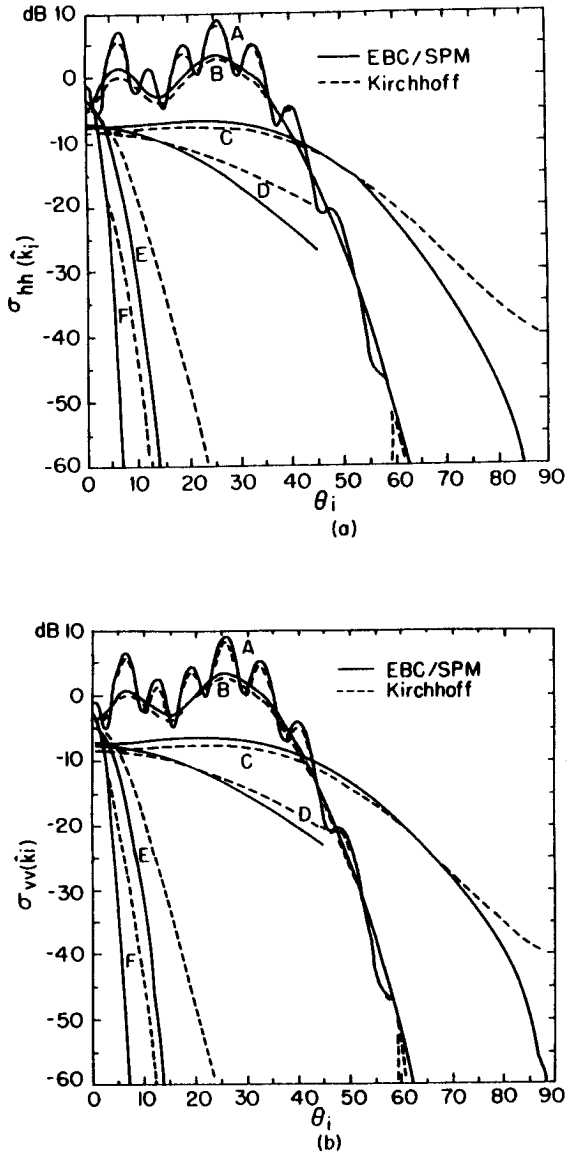

Figure 4.2.4 Backscattering cross section per unit area for various correlation lengths $l = 10$, 50, 100 cm with $\sigma = 1$ cm, $H = 10$ cm, $P = 100$ cm, $f = 1.4$ GHz and $\epsilon_1 = (6.0+i0.6)\epsilon_o$. (a) σ_{hh} versus θ_i with $\phi_i = 0°$ and 90°. (b) σ_{vv} versus θ_i with $\phi_i = 0°$and 90°. (Curves A: $l = 100$ cm, $\phi_i = 0°$; B: $l = 50$ cm, $\phi_i = 0°$; C: $l = 10$ cm, $\phi_i = 0°$; D: $l = 100$ cm, $\phi_i = 90°$; E: $l = 50$ cm, $\phi_i = 90°$; F: $l = 10$ cm, $\phi_i = 90°$); (——EBC/SPM, – – –Kirchhoff).

Oliner, 1965]: Floquet mode 2 becomes evanescent, and Floquet mode -3 becomes radiating at 11.5° and, similarly, for Floquet mode 1 and Floquet mode -4 at 36.9° in Ref. 2. Because of the roughness on the top of the periodic surface, even though the surface is illuminated by a plane wave with single spatial frequency, the surface currents and scattered fields of all spatial frequencies can be generated. The scattered fields with the same spatial frequencies as those of Wood's anomalies [Hessel and Oliner, 1965] will interact strongly with the periodic surface. This shows that the first-order scattered field pattern preserves every scattering characteristic of the periodic surface which is slightly different from those of the horizontally polarized incidence case as shown in Fig. 4.2.2.

The theoretical results for backscattering cross sections per unit area are illustrated in Figs. 4.2.4 and 4.2.5. This case has also been studied using the Kirchhoff approximation in [Shin and Kong, 1984], and the parameters used correspond to a typical terrain plow field.

In Fig. 4.2.4, the backscattering cross sections per unit area are plotted as a function of incident angle θ_i for azimuth angles $\phi_i = 0°$ and 90° and for correlation lengths $l = 10$, 50, and 100 cm. The results obtained from Kirchhoff approximation [Shin and Kong, 1984] show very good agreement with the results obtained using the EBC/SPM method at small angles of incidence. When the results in Fig. 4.2.4(a) are compared with those in Fig. 4.2.4(b), the EBC/SPM method gives different returns for σ_{hh} and σ_{vv} while the Kirchhoff approximation gives the identical results for both like-polarized returns. However, the difference between σ_{hh} and σ_{vv} is seen to be small. In Fig. 4.2.4 we note that several peaks show up for the large correlation length case where the incident angles satisfy the Bragg diffraction condition [Shin and Kong, 1984]

$$2k_{xi} = n2\pi/P \tag{46}$$

When the above condition is satisfied, the backscattering direction is coincident with the zeroth-order diffracted mode.

In Fig. 4.2.5, the backscattering cross sections per unit area are plotted as a function of azimuth incidence angle ϕ_i for $\theta_i = 25°$. The results for the horizontally and vertically polarized incidence are shown in Figs. 4.2.5(a) and 4.2.5(b), respectively. Again, we note a good agreement for σ_{hh} and σ_{vv} between Kirchhoff approximation and EBC/SPM method. However, the Kirchhoff approximation does

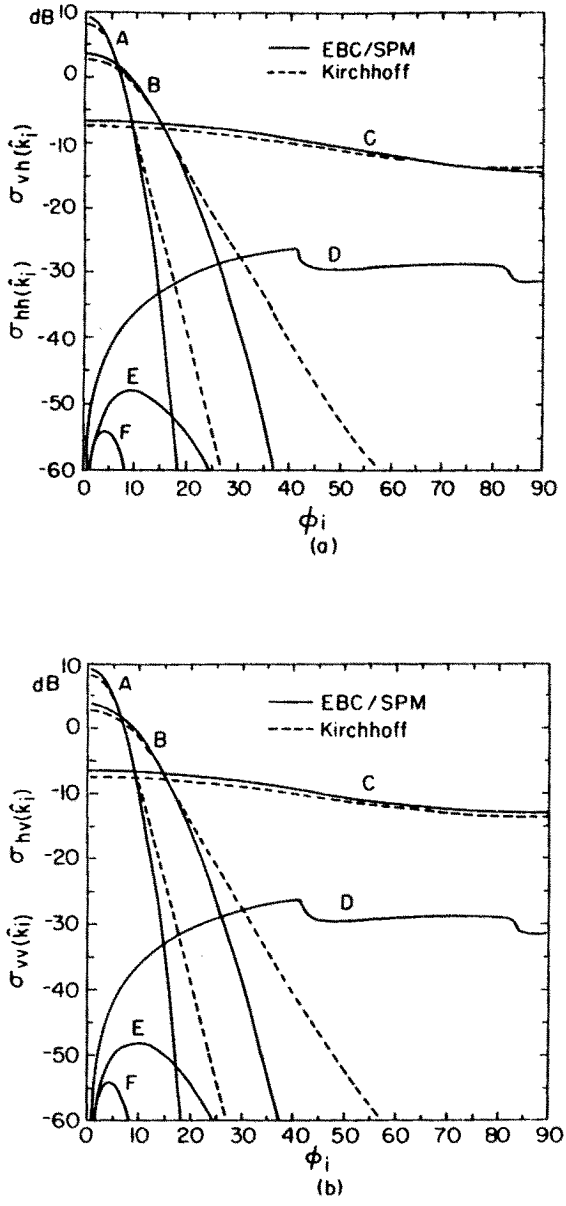

Figure 4.2.5 Backscattering cross section per unit area for various correlation lengths $l = 10, 50, 100$ cm with $\sigma = 1$ cm, $H = 10$ cm, $P = 100$ cm, $f = 1.4$ GHz and $\epsilon_1 = (6.0 + i0.6)\epsilon_o$. (a) σ_{hh} and σ_{vh} versus ϕ_i with $\theta_i = 25°$. (b) σ_{vv} and σ_{hv} versus ϕ_i with $\theta_i = 25°$. (Curves A: $l = 100$ cm, σ_{hh} or σ_{vv}; B: $l = 50$ cm, σ_{hh} or σ_{vv}; C: $l = 10$ cm, σ_{hh} or σ_{vv}; D: $l = 100$ cm, σ_{vh} or σ_{hv}; E: $l = 50$ cm, σ_{vh} or σ_{hv}; F: $l = 10$ cm, σ_{vh} or σ_{hv}); (——EBC/SPM, – – –Kirchhoff).

not give cross-polarized returns σ_{vh} in Fig. 4.2.5(a) and σ_{hv} in Fig. 4.2.5(b). The reason is that Kirchhoff approximation [Shin and Kong, 1984] makes use of the tangent plane approximation where the original rough surface can be seen as being approximated by many connected and locally perturbed tangent planes. Since it is well known that there is no cross-polarization in the first-order backscattering return from a randomly perturbed planar surface [Tsang et al., 1985], therefore Kirchhoff approximation predicts no depolarization in the backscattering direction. In this paper, the EBC/SPM method takes into account the curvature and tilting effect of the large-scale periodic surface exactly, and does give cross-polarized returns which can be significant when the incident wave vector is not perpendicular to the row directions. At $\phi_i \simeq 41°$ and $\phi_i \simeq 83°$ in the cross-polarized return (curve D: $l = 10$ cm), we can see two drops which correspond to the Rayleigh wavelength anomalies [Hessel and Oliner, 1965]: Floquet modes 3 and 4 become radiating modes at $\phi_i = 41.32°$ and $\phi_i = 83.13°$, respectively. Finally we note that the cross-polarized returns σ_{vh} and σ_{hv} presented in Figs. 4.2.5(a) and 4.2.5(b) are equal, which is consistent with the principle of reciprocity for the backscattering of electromagnetic wave from a reciprocal medium.

4.3 Scattering by a Randomly Perturbed Quasiperiodic Surface

a. Formulation

Consider a plane wave incident on a randomly perturbed quasiperiodic surface (Fig. 4.3.1). The electric field of the incident wave is given by

$$\overline{E}_i(\overline{r}) = \hat{e}_i E_o \exp(i\overline{k}_i \cdot \overline{r}) \tag{1}$$

where $\overline{k}_i$ denotes the incident wave vector and $\hat{e}_i$ the polarization of the incident electric field vector. The rough surface is characterized by a height distribution $Z = f(x,y)$, which is given by

$$f(x,y) = \xi(x,y) + A(x)\cos\left(\frac{2\pi}{P}x + \psi(x)\right) + B\cos\left(\frac{2\pi}{P}x + \phi\right) \tag{2}$$

where $\xi(x,y)$ is a Gaussian random variable with zero mean

$$\langle \xi(x,y) \rangle = 0 \tag{3}$$

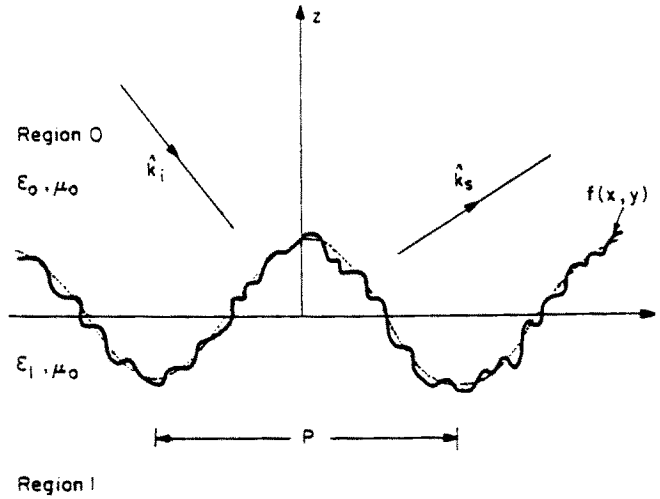

Figure 4.3.1 Geometrical configuration of the problem.

$A(x)\cos[(2\pi/P)x+\psi(x)]$ is described by a narrow-band Gaussian random process [Davenport and Root, 1958; Appendix D] centered around the spatial frequency of $2\pi/P$ where the variations of the envelope $A(x)$ and the phase $\psi(x)$ are slow compared to those of $\cos(2\pi x/P)$, and B and ϕ are assumed to be constants. Using the vector Kirchhoff approach, the scattered electric field $\overline{E}_s(\overline{r})$ can be expressed in the following form [Stogryn, 1967; Sancer, 1969; Leader, 1971; Tsang and Kong, 1980a]:

$$\overline{E}_s(\overline{r}) = \frac{ik\exp(ikr)}{4\pi r} E_o(\overline{I} - \hat{k}_s\hat{k}_s) \int_{A_o} \overline{F}(\alpha,\beta)\exp(i\overline{k}_d\cdot\overline{r}')d\overline{r}'_\perp \tag{4}$$

where A_o is the area of the rough surface projected onto the $x-y$ plane, $\hat{k}_s$ is the unit vector in the observation direction, and

$$\overline{k}_d = \overline{k}_i - \overline{k}_s \tag{5}$$

$$\begin{aligned}\overline{F}(\alpha,\beta) = (1+\alpha^2+\beta^2)^{1/2}\Big\{&-(1-R_h)(\hat{n}\cdot\hat{k}_i)(\hat{e}_i\cdot\hat{q}_i)\hat{q}_i \\ &+(\hat{e}_i\cdot\hat{p}_i)(\hat{n}\times\hat{q}_i)(1+R_v)+(\hat{e}_i\cdot\hat{q}_i)[\hat{k}_s\times(\hat{n}\times\hat{q}_i)](1+R_h) \\ &+(\hat{e}_i\cdot\hat{p}_i)(\hat{n}_i\cdot\hat{k}_i)(\hat{k}_s\times\hat{q}_i)(1-R_v)\Big\}\end{aligned} \tag{6}$$

In (6), α and β are the local slopes in the x and y directions,

$$\alpha = \frac{\partial f(x', y')}{\partial x'} \tag{7a}$$

$$\beta = \frac{\partial f(x', y')}{\partial y'} \tag{7b}$$

$\hat{n}$ is the local normal to the rough surface,

$$\hat{n} = \frac{-\hat{x}\alpha - \hat{y}\beta + \hat{z}}{(1 + \alpha^2 + \beta^2)^{1/2}} \tag{8}$$

$\hat{p}_i$ and $\hat{q}_i$ are, respectively, the unit vectors in the directions of the local parallel and perpendicular polarizations of the incident wave,

$$\hat{q}_i = \frac{\hat{k}_i \times \hat{n}}{|\hat{k}_i \times \hat{n}|} \tag{9a}$$

$$\hat{p}_i = \hat{q}_i \times \hat{k}_i \tag{9b}$$

R_v and R_h are the Fresnel reflection coefficients for TM and TE waves with local incidence angle:

$$R_h = \frac{-(\hat{n} \cdot \hat{k}_i) - [n_1^2 - 1 + (\hat{n} \cdot \hat{k}_i)^2]^{1/2}}{-(\hat{n} \cdot \hat{k}_i) + [n_1^2 - 1 + (\hat{n} \cdot \hat{k}_i)^2]^{1/2}} \tag{10a}$$

$$R_v = \frac{-n_1^2(\hat{n} \cdot \hat{k}_i) - [n_1^2 - 1 + (\hat{n} \cdot \hat{k}_i)^2]^{1/2}}{-n_1^2(\hat{n} \cdot \hat{k}_i) + [n_1^2 - 1 + (\hat{n} \cdot \hat{k}_i)^2]^{1/2}} \tag{10b}$$

with

$$\begin{aligned} n_1 &= k_1/k \\ k_1 &= \omega\sqrt{\mu_o \epsilon_1} \\ k &= \omega\sqrt{\mu_o \epsilon_o} \end{aligned} \tag{11}$$

and the orthonormal system for the incident and scattered fields are given by

$$\hat{k}_i = \hat{x} \sin\theta_i \cos\phi_i + \hat{y} \sin\theta_i \sin\phi_i - \hat{z} \cos\theta_i \tag{12a}$$

$$\hat{h}_i = -\hat{x} \sin\phi_i + \hat{y} \cos\phi_i \tag{12b}$$

$$\hat{v}_i = -\hat{x} \cos\theta_i \cos\phi_i - \hat{y} \cos\theta_i \sin\phi_i - \hat{z} \sin\theta_i \tag{12c}$$

$$\hat{k}_s = \hat{x} \sin\theta_s \cos\phi_s + \hat{y} \sin\theta_s \sin\phi_s + \hat{z} \cos\theta_s \tag{13a}$$

$$\hat{h}_s = -\hat{x} \sin\phi_s + \hat{y} \cos\phi_s \tag{13b}$$

$$\hat{v}_s = \hat{x} \cos\theta_s \cos\phi_s + \hat{y} \cos\theta_s \sin\phi_s - \hat{z} \sin\theta_s \tag{13c}$$

The Kirchhoff approximated diffraction integral in its present form is still difficult to evaluate, and further approximation is necessary. One commonly used approximation is to expand $\overline{F}(\alpha,\beta)$ in the power series of slope terms about the zero slope and to keep only the first few terms [Leader, 1971; Tsang and Newton, 1982]. However, in this section we shall expand $\overline{F}(\alpha,\beta)$ about the slopes at the stationary phase point α_o and β_o,

$$\alpha_o = -\frac{k_{dx}}{k_{dz}} \tag{14a}$$

$$\beta_o = -\frac{k_{dy}}{k_{dz}} \tag{14b}$$

where

$$k_{dx} = k(\sin\theta_i \cos\phi_i - \sin\theta_s \cos\phi_s) \tag{15a}$$

$$k_{dy} = k(\sin\theta_i \sin\phi_i - \sin\theta_s \sin\phi_s) \tag{15b}$$

$$k_{dz} = -k(\cos\theta_i + \cos\theta_s) \tag{15c}$$

Therefore, we expand $\overline{F}(\alpha,\beta)$ as follows:

$$\overline{F}(\alpha,\beta) = \overline{F}(\alpha_o,\beta_o) + \left.\frac{\partial \overline{F}}{\partial \alpha}\right|_{\alpha_o\beta_o} (\alpha-\alpha_o) + \left.\frac{\partial \overline{F}}{\partial \beta}\right|_{\alpha_o\beta_o} (\beta-\beta_o) + \cdots \tag{16}$$

Keeping only the first term in the above equation, we obtain from (4),

$$\overline{E}_s(\overline{r}) = \frac{ik\exp(ikr)}{4\pi r} E_o(\overline{I} - \hat{k}_s\hat{k}_s)\overline{F}(\alpha_o,\beta_o)I \tag{17}$$

where the integral I is given by

$$I = \int_{A_o} \exp(i\overline{k}_d \cdot \overline{r}')d\overline{r}'_\perp \tag{18}$$

Then the scattered field $\overline{E}_s(\overline{r})$ is separated into a mean field $\overline{E}_m(\overline{r})$ and a fluctuating part of the field $\overline{\mathcal{E}}(\overline{r})$

$$\overline{E}_s(\overline{r}) = \overline{E}_m(\overline{r}) + \overline{\mathcal{E}}(\overline{r}) \tag{19}$$

with

$$\langle\overline{\mathcal{E}}(\overline{r})\rangle = 0 \tag{20}$$

and

$$\langle \overline{E}_s(\bar{r}) \rangle = \overline{E}_m(\bar{r}) \tag{21}$$

so that the total scattered intensity is a sum of coherent and incoherent scattered intensities.

$$\langle |\overline{E}_s|^2 \rangle = |\overline{E}_m(\bar{r})|^2 + \langle |\overline{\mathcal{E}}(\bar{r})|^2 \rangle \tag{22}$$

From (17) and (18), we have

$$\langle |\overline{E}_m(\bar{r})|^2 \rangle = \frac{k^2 |E_o|^2}{16\pi^2 r^2} \left[|\hat{v}_s \cdot \overline{F}(\alpha_o, \beta_o)|^2 + |\hat{h}_s \cdot \overline{F}(\alpha_o, \beta_o)|^2 \right] |\langle I \rangle|^2 \tag{23}$$

and

$$\langle |\overline{\mathcal{E}}(\bar{r})|^2 \rangle = \frac{k^2 |E_o|^2}{16\pi^2 r^2} \left[|\hat{v}_s \cdot \overline{F}(\alpha_o, \beta_o)|^2 + |\hat{h}_s \cdot \overline{F}(\alpha_o, \beta_o)|^2 \right] D_I \tag{24}$$

where

$$D_I = \langle |I|^2 \rangle - |\langle I \rangle|^2 \tag{25}$$

The explicit expressions for $|\langle I \rangle|^2$ and D_I for the randomly perturbed quasiperiodic surface are derived and expressed in terms of the statistical moments of the height distribution [Appendix E]. The advantage of expanding $\overline{F}(\alpha, \beta)$ around the stationary phase point (α_o, β_o) is that the bistatic scattering coefficients derived from (24) and (25) satisfy the principle of reciprocity, and at high frequency limit the geometrical optics solutions can be obtained from (25) without making any modifications [Stogryn, 1967]. Also, since $\overline{F}(\alpha, \beta)$ is evaluated at the stationary phase point, the same solution is obtained using total or reflected field on the surface [Holzer and Sung, 1978].

b. Coherent and Incoherent Scattering Coefficients

The bistatic scattering coefficients are defined as [Peake, 1959]

$$\gamma_{ab}(\hat{k}_s, \hat{k}_i) = \frac{4\pi r^2 I_{sa}}{A_o \cos\theta_i I_{ib}} \qquad (a, b = v, h) \tag{26}$$

where I_{sa} and I_{ib} are, respectively, the intensity of the scattered wave in polarization a and the intensity of the incident wave in polarization b. From (23) and (24) we first calculate the vertically and horizontally polarized coherent and incoherent scattered intensities for the cases of vertically and horizontally polarized incident fields. For an incident

field with polarization b_i, the scattered intensities with polarization a_s are given by [Stogryn, 1967]

$$|E_m(\bar{r})|^2 = \frac{k^2 |E_o|^2}{16\pi^2 r^2} \left|\hat{a}_s \cdot \overline{F}_b(\alpha_o, \beta_o)\right|^2 |\langle I \rangle|^2 \tag{27}$$

$$|\mathcal{E}(\bar{r})|^2 = \frac{k^2 |E_o|^2}{16\pi^2 r^2} \left|\hat{a}_s \cdot \overline{F}_b(\alpha_o, \beta_o)\right|^2 D_I \tag{28}$$

where

$$\overline{F}_b(\alpha_o, \beta_o) = \overline{F}(\alpha_o, \beta_o)\big|_{\hat{e}_i = \hat{b}_i} \tag{29}$$

and

$$\left|\hat{a}_s \cdot \overline{F}_b(\alpha_o, \beta_o)\right|^2 = \frac{\left|\overline{k}_d\right|^4}{k^2 \left|\hat{k}_i \times \hat{k}_s\right|^4 k_{dz}^2} f_{ba} \tag{30}$$

with

$$f_{vv} = \left|(\hat{h}_s \cdot \hat{k}_i)(\hat{h}_i \cdot \hat{k}_s) R_h + (\hat{v}_s \cdot \hat{k}_i)(\hat{v}_i \cdot \hat{k}_s) R_v\right|^2 \tag{31a}$$

$$f_{vh} = \left|(\hat{h}_s \cdot \hat{k}_i)(\hat{v}_i \cdot \hat{k}_s) R_h - (\hat{v}_s \cdot \hat{k}_i)(\hat{h}_i \cdot \hat{k}_s) R_v\right|^2 \tag{31b}$$

$$f_{hv} = \left|(\hat{v}_s \cdot \hat{k}_i)(\hat{h}_i \cdot \hat{k}_s) R_h - (\hat{h}_s \cdot \hat{k}_i)(\hat{v}_i \cdot \hat{k}_s) R_v\right|^2 \tag{31c}$$

$$f_{hh} = \left|(\hat{v}_s \cdot \hat{k}_i)(\hat{v}_i \cdot \hat{k}_s) R_h + (\hat{h}_s \cdot \hat{k}_i)(\hat{h}_i \cdot \hat{k}_s) R_v\right|^2 \tag{31d}$$

and R_v and R_h, which are given by (10), are evaluated at

$$\hat{n} = \frac{\hat{x} k_{dx}/k_{dz} + \hat{y} k_{dy}/k_{dz} + \hat{z}}{(k_{dx}^2/k_{dz}^2 + k_{dy}^2/k_{dz}^2 + 1)^{1/2}} \tag{32}$$

In view of (27) and (28), the bistatic scattering coefficients can be decomposed into a coherent part γ_{ab}^c and an incoherent part γ_{ab}^i. Substituting in the expressions for $|\langle I \rangle|^2$ and D_I, (E10) and (E18), into (27) and (28), we have

$$\gamma_{ab}(\hat{k}_s, \hat{k}_i) = \gamma_{ab}^c(\hat{k}_s, \hat{k}_i) + \gamma_{ab}^i(\hat{k}_s, \hat{k}_i) \tag{33}$$

where

$$\gamma_{ab}^{c}(\hat{k}_s, \hat{k}_i) = \frac{\pi |\bar{k}_d|^4}{\cos\theta_i \left|\hat{k}_i \times \hat{k}_s\right|^4 k_{dz}^2} f_{ba} \exp[-k_{dz}^2(\sigma^2 + \sigma_x^2)] \times \sum_{n=-\infty}^{\infty} |J_n(k_{dz}B)|^2 \delta\left(k_{dx} + n\frac{2\pi}{P}\right) \delta(k_{dy}) \tag{34}$$

$$\gamma_{ab}^{i}(\hat{k}_s, \hat{k}_i) = \frac{|\bar{k}_d|^4}{\cos\theta_i k^2 \left|\hat{k}_i \times \hat{k}_s\right|^4 k_{dz}^2} f_{ba} (D_{I_1} + D_{I_2}) \tag{35}$$

In (34), J_n is the nth-order Bessel function, and δ is the Dirac delta function. It can easily be shown that the bistatic scattering coefficients satisfy the principle of reciprocity,

$$\cos\theta_i \gamma_{ab}(\hat{k}_s, \hat{k}_i) = \cos\theta_s \gamma_{ba}(\hat{k}_i, \hat{k}_s) \tag{36}$$

When the incident wave vector is not perpendicular to the row direction of the periodic surface ($k_{yi} \neq 0$), the coherent scattering coefficient, (34), gives rise to scattered intensities along the directions of Floquet modes, forming a cone. This conical diffraction is a characteristic of scattering from a periodic surface [Chuang and Kong, 1982]. A part of incoherent scattering coefficient will also give rise to conical diffraction. The second term on the right-hand side of (35) has $\delta(k_{dy})$ dependence, and this will give rise to scattered intensities only in the direction $k_{ys} = k_{yi}$ forming a cone shape. However, unlike the coherent term, which only scatters into a set of discrete directions, this term will scatter intensities in all k_{xs} directions.

In the backscattering direction $\theta_s = \theta_i$ and $\phi_s = \phi_i + \pi$. The backscattering cross sections per unit area are defined to be

$$\sigma_{ab}(\hat{k}_i) = \cos\theta_i \gamma_{ab}(-\hat{k}_i, \hat{k}_i) \tag{37}$$

From (33)–(35) we obtain

$$\sigma_{vv}(\hat{k}_i) = \sigma_{hh}(\hat{k}_i) = \sigma^c(\hat{k}_i) + \sigma_1^i(\hat{k}_i) + \sigma_2^i(\hat{k}_i) \tag{38}$$

$$\sigma_{hv}(\hat{k}_i) = \sigma_{vh}(\hat{k}_i) = 0 \tag{39}$$

where

$$\sigma^c(\hat{k}_i) = \frac{4\pi k^2 |R|^2}{\cos^2\theta_i} \exp\left[-4k_{zi}^2(\sigma^2 + \sigma_x^2)\right] \sum_{n=-\infty}^{\infty} |J_n(2k_{zi}B)|^2 \times \delta\left(2k_{xi} + n\frac{2\pi}{P}\right) \delta(2k_{yi}) \tag{40}$$

$$\sigma_1^i(\hat{k}_i) = \frac{k^2 |R|^2}{\cos^2\theta_i} \sum_{\mu=-\infty}^{\infty} |J_n(2k_{zi}B)|^2 \exp\left[-4k_{zi}^2(\sigma^2 + \sigma_x^2)\right] \times \sum_{m=1}^{\infty} \frac{(4k_{zi}^2\sigma^2)^m}{m!} \frac{l^2}{m} \left[\exp\left(-\left[\left(\frac{k_{xi} + \mu\pi}{P}\right)^2 + k_{yi}^2\right]\frac{l^2}{m}\right) + \sum_{m'=1}^{\infty} \sum_{n=0}^{m'} \frac{1}{2^{m'}} \binom{m'}{n} \frac{(4k_{zi}^2\sigma_x^2)^{m'}}{m'!} \frac{1}{q} \times \exp\left(-\left[\frac{k_{xi} + (\mu + m' - 2n)\pi}{P}\right]^2 \frac{l^2}{mq} - k_{yi}^2 \frac{l^2}{m}\right)\right] \tag{41}$$

with

$$q = \sqrt{1 + \frac{l^2 m'}{l_x^2 m}}$$

$$\sigma_2^i(\hat{k}_i) = \frac{2k^2 |R|^2}{\cos^2\theta_i} \delta(2k_{yi}) \sum_{\mu=-\infty}^{\infty} |J_n(2k_{zi}B)|^2 \exp\left[-4k_{zi}^2(\sigma^2 + \sigma_x^2)\right] \times \sum_{m=1}^{\infty} \sum_{n=0}^{m} \frac{1}{2^m} \binom{m}{n} \sqrt{\frac{\pi}{m}} l_x \frac{(4k_{zi}^2\sigma_x^2)^m}{m!} \times \exp\left(-\left[\frac{k_{xi} + (\mu + m - 2n)\pi}{P}\right]^2 \frac{l_x^2}{m}\right) \tag{42}$$

and R is the Fresnel reflection coefficient at normal incidence. We note that there is no depolarization in the backscattering direction, and because of the $\delta(2k_{yi})$ dependence, $\sigma^c(\hat{k}_i)$ terms contribute only when the incident wave vector is perpendicular to the row direction of the periodic surface.

c. *Geometrical Optics Solution*

Under the geometrical optics limit as $k \to \infty$, further simplifications can be made for the expressions of $|\langle I \rangle|^2$ and D_I. Since $k_{dz}\sigma, k_{dz}\sigma_x \gg 1$, the coherent component of the scattered fields are negligible, and only the incoherent scattering coefficients will remain. Under the stationary phase approximation the bistatic scattering coefficients simplify to

$$\gamma_{ab}(\hat{k}_s, \hat{k}_i) = \frac{|\bar{k}_d|^4}{\cos\theta_i \left|\hat{k}_i \times \hat{k}_s\right|^4 k_{dz}^4} f_{ba} \frac{1}{2\pi} \int_0^{2\pi} d\phi' \frac{1}{2s_x s_y} \exp\left(-\frac{\left(\frac{k_{dx}}{k_{dz}} - 2\pi\frac{B}{P}\sin\phi'\right)^2}{2s_x^2} - \frac{\left(\frac{k_{dy}}{k_{ds}}\right)^2}{2s_y^2} \right) \tag{43}$$

where s_x^2 and s_y^2 are, respectively, the mean square surface slopes in the x and y directions

$$s_x^2 = \sigma^2 |C''(0)| + \sigma_x^2[(2\pi/P)^2 + |C_x''(0)|] \tag{44a}$$

$$s_y^2 = \sigma^2 |C''(0)| \tag{44b}$$

In the above equations, C'' and C_x'' are the second derivatives of the correlation functions and for Gaussian correlation functions assumed

$$|C''(0)| = 2/l^2 \tag{45a}$$

$$|C_x''(0)| = 2/l_x^2 \tag{45b}$$

The probability of finding slopes (α, β) at point $\bar{r}_\perp$ on the surface can be calculated to be

$$P[\alpha(\bar{r}_\perp), \beta(\bar{r}_\perp)] = \frac{1}{2\pi s_x s_y} \exp\left(-\frac{\left[\alpha + 2\pi\frac{B}{P}\sin\left(\frac{2\pi}{P}x + \phi\right)\right]^2}{2s_x^2} - \frac{\beta^2}{2s_y^2} \right) \tag{46}$$

Averaging the above expression over one period we obtain the averaged PDF for α, β

$$P(\alpha, \beta) = \frac{1}{P} \int_0^P dx \frac{1}{2\pi s_x s_y} \exp\left(-\frac{\left[\alpha + 2\pi\frac{B}{P}\sin\left(\frac{2\pi}{P}x + \phi\right)\right]^2}{2s_x^2} - \frac{\beta^2}{2s_y^2} \right) \tag{47}$$

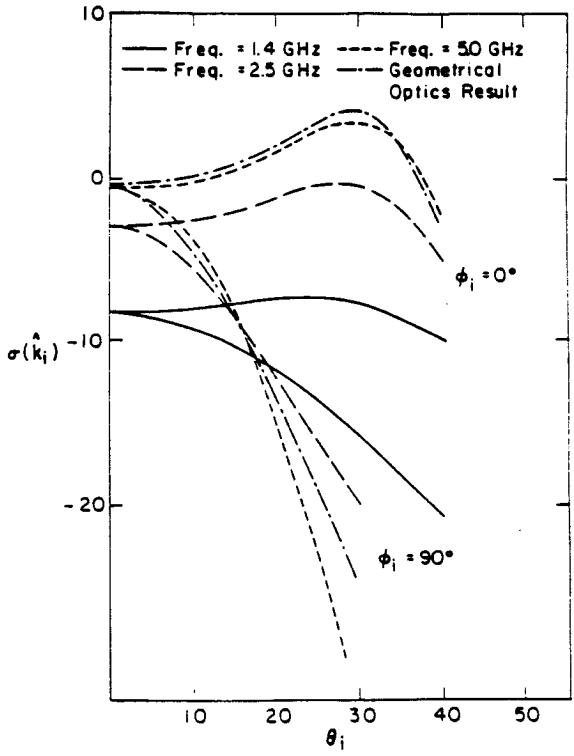

Figure 4.3.2 $\sigma(\hat{k}_i)$ **as a function of** θ_i **for different frequencies with** $\sigma =$ **1 cm,** $l = 10$ **cm,** $B = 10$ **cm,** $P = 100$ **cm,** $\sigma_x = 0$, **and** $\epsilon_1 = (6.0 + i0.6)\epsilon_o$.

which is proportional to the geometrical optics solution. Therefore, the geometrical optics result states that the scattered intensity is proportional to the probability of the occurrence of the slopes which will specularly reflect the incident wave into the direction of the scattered wave [Barrick, 1968]. We also note that in the geometrical optics limit there is no difference between the above solution and the solution obtained using the incoherent model [Ulaby *et al.*, 1982] except for the factors due to quasiperiodicity.

d. Results and Discussion

The backscattering cross sections per unit area $\sigma_1^i(\hat{k}_i)$ are calculated and illustrated for various cases. The conically diffracted coherent

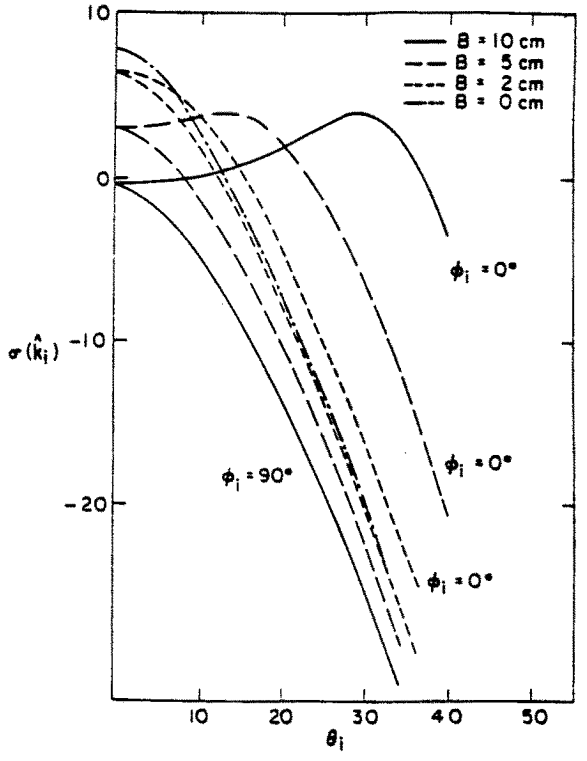

Figure 4.3.3 $\sigma(\hat{k}_i)$ **as a function of** θ_i **for different values of** B **at 5.0 GHz with** $P = 100$ **cm,** $\sigma = 1$ **cm,** $l = 10$ **cm,** $\sigma_x = 0$, **and** $\epsilon_1 = (6.0 + i0.6)\epsilon_o$.

and incoherent components, $\sigma^c(\hat{k}_i)$ and $\sigma_2^i(\hat{k}_i)$, which only contribute when the incident wave is perpendicular to the row direction of the periodic surface, are not included in the calculations. In order to correctly incorporate the contributions from these components, the characteristics of the antenna used to make the measurements must be taken into account.

The results of randomly perturbed sinusoidal surface cases, $\sigma_x = 0$, are first illustrated in Figs. 4.3.2–4.3.12. In Fig. 4.3.2, the backscattering cross sections per unit area $\sigma(\hat{k}_i)$ are plotted as a function of incidence angle for different frequencies. As the frequency is increased, the solution approaches the geometrical optics result as expected. The difference between the cases where the incident wave vector is parallel, $\phi_i = 90°$, or perpendicular, $\phi_i = 0°$, to the row direction is seen to

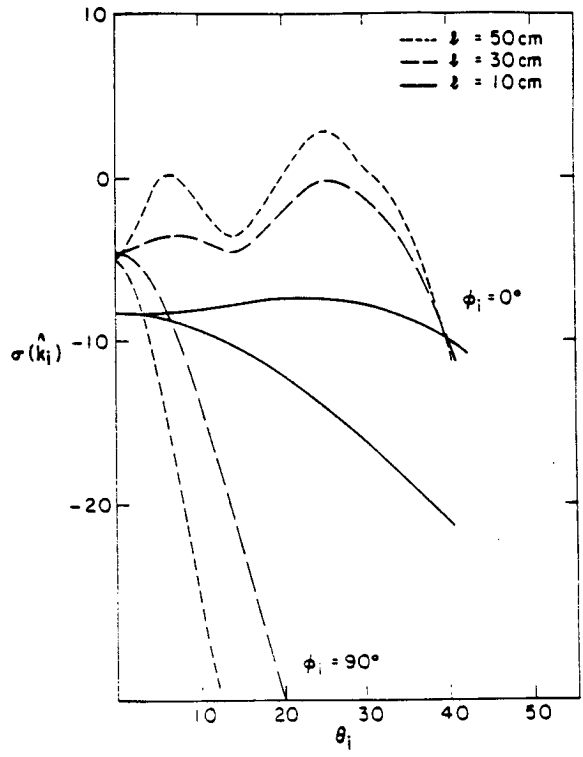

Figure 4.3.4 $\sigma(\hat{k}_i)$ **as a function of** θ_i **for different values of** l **at 1.4 GHz with** $\sigma = 1$ **cm,** $B = 10$ **cm,** $P = 100$ **cm,** $\sigma_x = 0$, **and** $\epsilon_1 = (6.0 + i0.6)\epsilon_o$.

be large. For the $\phi_i = 0°$ case the maximum value of $\sigma(\hat{k}_i)$ is shown to be not at normal incidence. In Fig. 4.3.3 the effect of change in the amplitude of sinusoidal variation B is illustrated for 5.0 GHz. As B is decreased the results of $\phi_i = 0°$ and $\phi_i = 90°$ cases approach each other, and when $B = 0$ we reproduce the random rough surface result which is independent of azimuthal incident angle ϕ_i.

In Fig. 4.3.4 the effect of the correlation length l at 1.4 GHz is illustrated. As l is increased, the $\sigma(\hat{k}_i)$ falls off faster as a function of θ_i for $\phi_i = 90°$, and there is an appearance of peaks for $\phi_i = 0°$. The change in $\sigma(\hat{k}_x)$ as ϕ_i is varied is shown in Fig. 4.3.5. The appearance of the peaks for $\phi_i = 0°$ can be explained as follows.

The result for a randomly perturbed sinusoidal surface is related to the convolution of the results for the sinusoidal surface with those of the

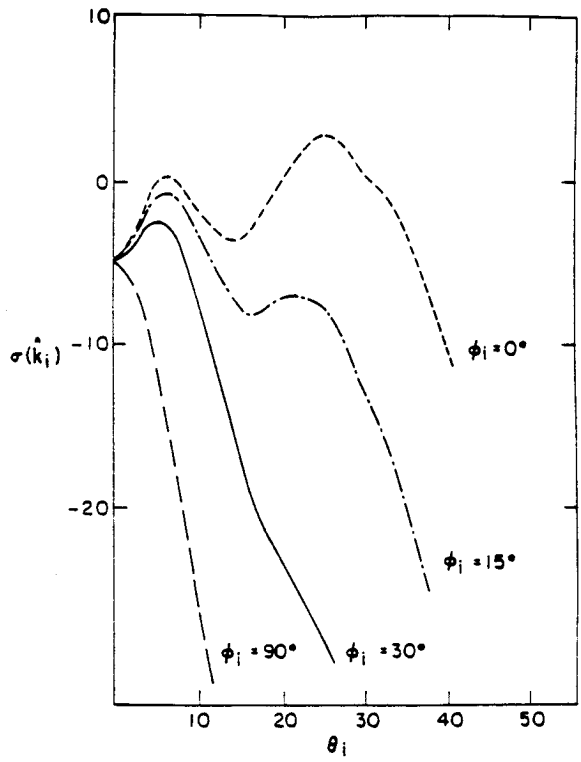

Figure 4.3.5 $\sigma(\hat{k}_i)$ **as a function of** θ_i **for different azimuthal angles of incidence** ϕ_i **at 1.4 GHz with** $\sigma = 1$ **cm,** $l = 50$ **cm,** $B = 10$ **cm,** $P = 100$ **cm,** $\sigma_x = 0$, **and** $\epsilon_1 = (6.0 + i0.6)\epsilon_o$.

random rough surface. For a sinusoidal surface, we have contribution in the backscattering direction only when it coincides with one of the Floquet modes direction.

$$2k_{xi} = n\frac{2\pi}{P} \tag{48}$$

As l is increased the scattering pattern from a random rough surface is sharply peaked around the specular direction. Therefore, by making l sufficiently large, we obtain the result which is sharply peaked at the mode directions given by (48). This is illustrated in Fig. 4.3.6(a). The locations and amplitudes of the Floquet modes are plotted in Fig. 4.3.6(a). Notice that for the cases of $l = 100\,\text{cm}$, we see from Fig.

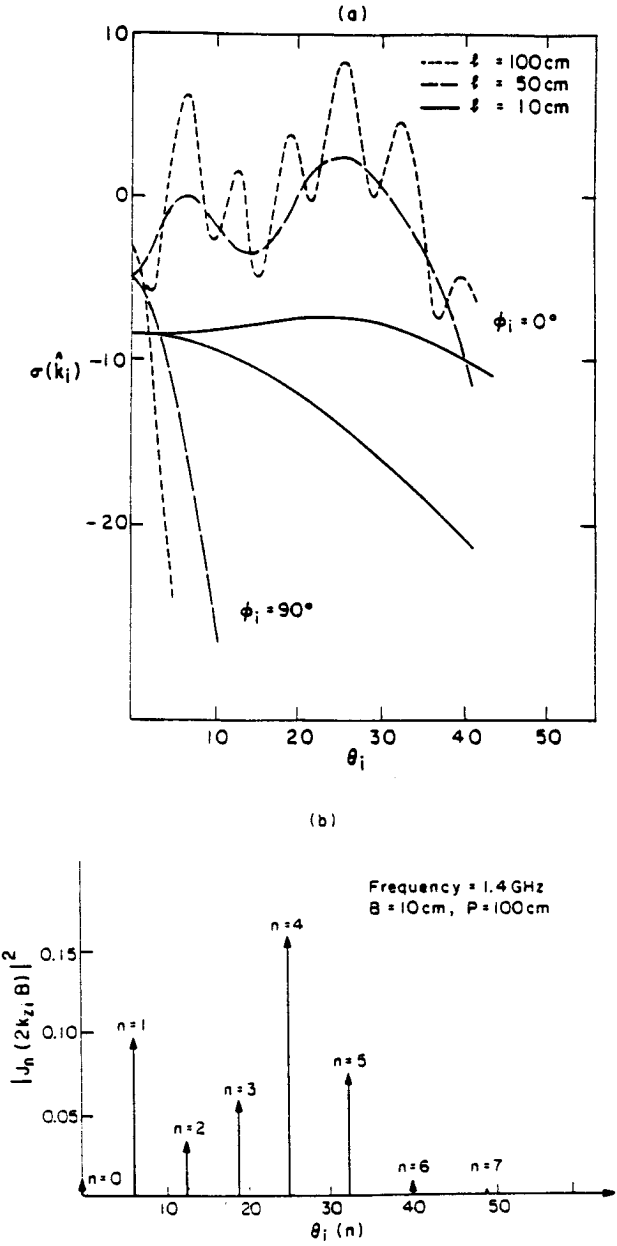

Figure 4.3.6 (a) $\sigma(\hat{k}_i)$ as a function of θ_i for different values of l at 1.4 GHz with $\sigma = 1$ cm, $B = 10$ cm, $P = 100$ cm, $\sigma_z = 0$, and $\epsilon_1 = (6.0 + i0.6)\epsilon_o$. (b) Locations and amplitudes of the modes for $B = 10$ cm.

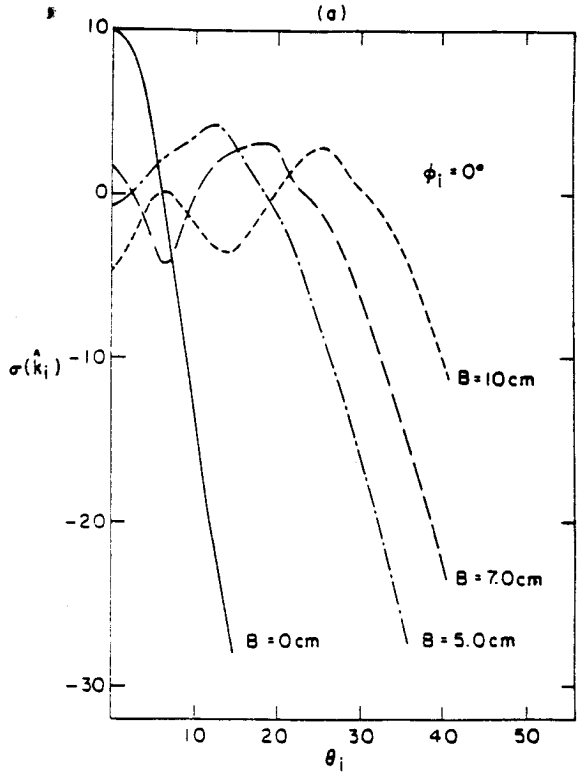

Figure 4.3.7 (a) $\sigma(\hat{k}_i)$ as a function of θ_i for different values of B at 1.4 GHz with $\sigma = 1$ cm, $l = 50$ cm, $P = 100$ cm, $\sigma_x = 0$, and $\epsilon_1 = (6.0+i0.6)\epsilon_o$.

4.3.6(a) that the peaks are visibly illustrated. When l is smaller the scattering pattern of the random rough surface becomes broader, and we do not reproduce all the peaks. However, the peaks around the two dominant modes, $n = 1$ and $n = 4$, are still reproduced for $l = 50$ cm. When l is further decreased none of the peaks are reproduced, and we have a fairly flat behavior.

In Fig. 4.3.7(a), the effect of change in B at 1.4 GHz is illustrated. Note that as B is decreased, there seems to be a shifting of the peaks. Since the period P is not changed, the locations of the modes do not change. However, as we can see from Fig. 4.3.7(b), the amplitude of each mode is changed as B is changed. The location of the mode with the maximum amplitude is shifted as B is varied, and the results in Fig. 4.3.7(a) reflect this effect. When $B = 0$ only the amplitude of

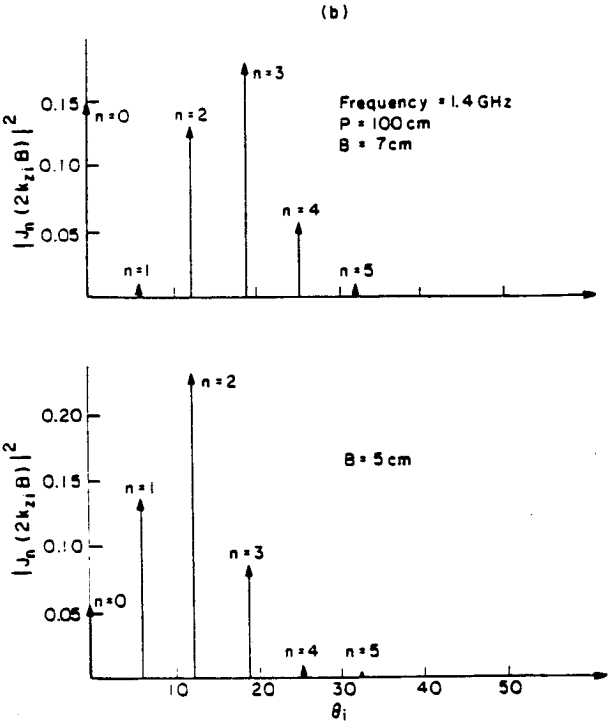

Figure 4.3.7 (b) Locations and amplitudes of the modes for $B = 7$ cm and $B = 5$ cm.

the $n = 0$ mode is nonzero, and the random rough surface result is reproduced.

The effect of change in the period P is illustrated in Fig. 4.3.8. The locations of the modes will change as P changes, while the amplitude of each mode will not change since B is the same. As can be seen from Fig. 4.3.8, when P is increased the modes are spaced closer together, and when P is decreased the modes become further apart.

The effect of change in σ is shown in Fig. 4.3.9(a). Initially, as σ is increased, the backscattering cross section $\sigma(\hat{k}_i)$ is increased. Then, as σ is further increased, there is a decrease near normal incidence and a disappearance of one of the peaks. This is due to the change in the scattering characteristics of the random rough surface in the absence of sinusoidal variation. In Fig. 4.3.9(b) the backscattering cross section

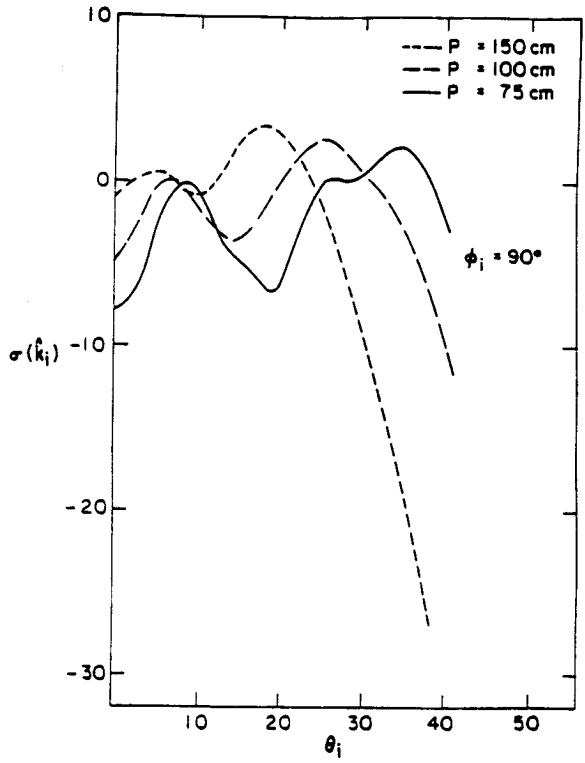

Figure 4.3.8 $\sigma(\hat{k}_i)$ **as a function of** θ_i **for different values of** P **at 1.4 GHz with** $\sigma = 1$ **cm,** $l = 50$ **cm,** $B = 10$ **cm,** $P = 100$ **cm,** $\sigma_x = 0$, **and** $\epsilon_1 = (6.0 + i0.6)\epsilon_o$.

for the random rough surface is plotted. Note that for $\sigma = 5\,\text{cm}$ there is a decrease near normal incidence and a broadening of the scattering pattern which explains the trends in Fig. 4.3.9(a).

In Fig. 4.3.10(a) and 4.3.10(b) we illustrate the results for randomly perturbed quasi-periodic surfaces, $B = 0$ and $\sigma_x \neq 0$. In Fig. 4.3.10(a) the backscattering cross sections are plotted for different correlation lengths l. Again, as l is increased, there is an appearance of peaks. But unlike the sinusoidal case, the values of the peaks are monotonically decreasing with increasing angle of incidence. It is interesting to look at the solution in the limit $l_x \to \infty$ since we obtain

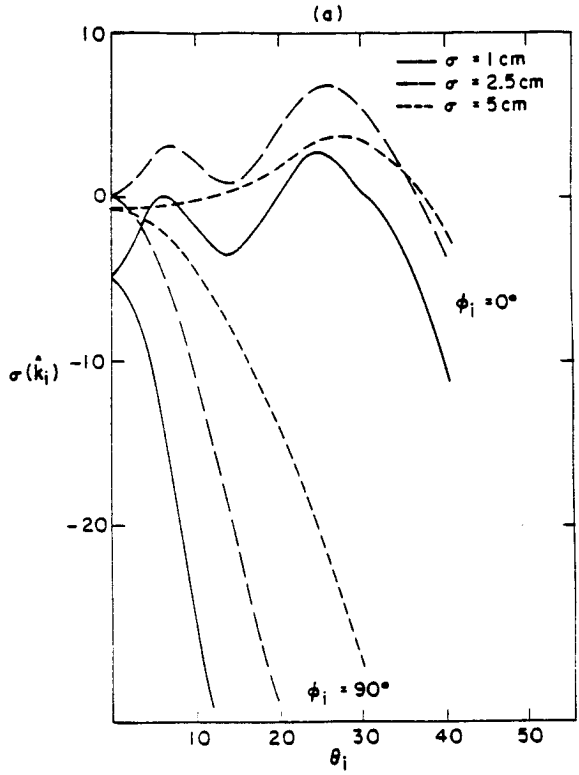

Figure 4.3.9 (a) $\sigma(\hat{k}_i)$ as a function of θ_i for different values of σ at 1.4 GHz with $l = 50$ cm, $B = 10$ cm, $P = 100$ cm, $\sigma_x = 0$, and $\epsilon_1 = (6.0 + i0.6)\epsilon_o$.

a much simpler analytical solution. From (E14) we obtain, for $B = 0$,

$$\langle II^* \rangle = \int_{-2L_x}^{2L_x} dx \int_{-2L_y}^{2L_y} dy\, e^{i\bar{k}_{d\perp}\cdot\bar{r}_\perp}[2L_x - |x|][2L_y - |y|] \exp\left[-k_{dz}^2\sigma^2 + k_{dz}^2\sigma^2 C(\bar{r}_\perp)\right] \times \exp\left[-k_{dz}^2\sigma_x^2 + k_{dz}^2\sigma_x^2 C_x(x)\right] \tag{49}$$

In the limit $l_x \to \infty$, we obtain

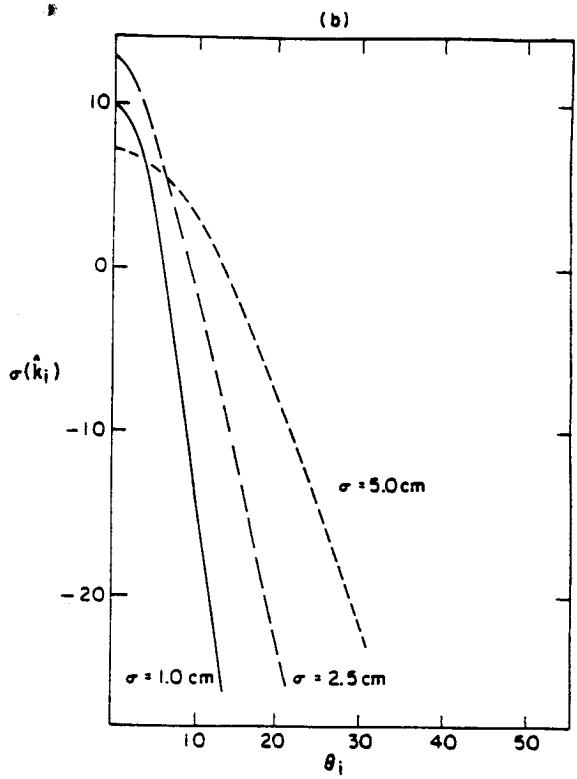

Figure 4.3.9 (b) $\sigma(\hat{k}_i)$ as a function of θ_i for different values of σ at 1.4 GHz with $l = 50$ cm, $B = 0$, $\sigma_x = 0$, and $\epsilon_1 = (6.0 + i0.6)\epsilon_o$.

$$\langle II^* \rangle = \int_{-2L_x}^{2L_x} dx \int_{-2L_y}^{2L_y} dy \sum_{n=-\infty}^{\infty} \exp\left[-k_{dz}^2\sigma_x^2\right] I_n(k_{dz}^2\sigma_x^2) \exp\left[i\left(\bar{k}_{d\perp} + \hat{x}n\frac{2\pi}{P}\right)\cdot\bar{r}_\perp\right] \times [2L_x - |x|][2L_y - |y|] \exp\left[-k_{dz}^2\sigma^2 + k_{dz}^2\sigma^2 C(\bar{r}_\perp)\right] \quad (50)$$

where I_n is the nth order modified Bessel function. This is similar to the randomly perturbed sinusoidal surface result. In this case the amplitudes of the modes are given by the modified Bessel functions, whereas before they were given in terms of the Bessel functions. The

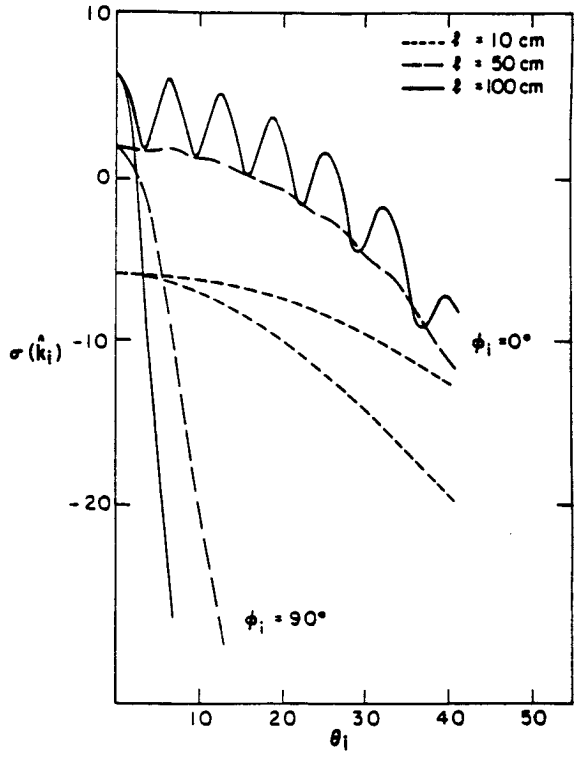

Figure 4.3.10 (a) $\sigma(\hat{k}_i)$ as a function of θ_i for different values of l at 1.4 GHz with $\sigma = 1$ cm, $B = 0$, $P = 100$ cm, $\sigma_x = 5$ cm, $l_x = 300$ cm, and $\epsilon_1 = (6.0 + i0.6)\epsilon_o$.

amplitudes of the modes are plotted in Fig. 4.3.10(b), and we can see that they are monotonically decreasing as n is increased, which explains the results in Fig. 4.3.10(a). Also note that as σ_x is decreased, only the first few modes have larger amplitudes; and as n is increased, they decay much faster. When $\sigma_x = 0$, only the $n = 0$ mode remains, and we reproduce the random rough surface results.

The above result in the limit $\sigma_x \to \infty$, (50), can also be related to the randomly perturbed sinusoidal surface case. When $\sigma_x = 0$, we obtain

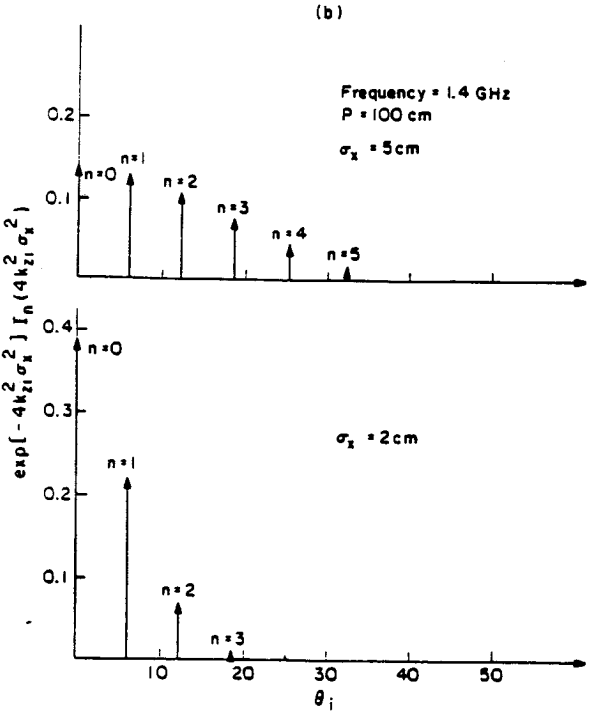

Figure 4.3.10 (b) Locations and amplitudes of the modes for $\sigma_x = 5$ cm and $\sigma_x = 2$ cm.

$$\langle II^* \rangle = \int_{-2L_x}^{2L_x} dx \int_{-2L_y}^{2L_y} dy \sum_n J_n^2(k_{dz}B) \exp\left[i\left(\bar{k}_{d\perp} + \hat{x}n\frac{2\pi}{P}\right)\cdot\bar{r}_\perp\right]$$
$$\times [2L_x - |x|][2L_y - |y|] \exp\left[-k_{dz}^2\sigma^2 + k_{dz}^2\sigma^2 C(\bar{r}_\perp)\right] \qquad (51)$$

For a narrow-band Gaussian random process, $A(x)\cos[(2\pi/P)x + \psi(x)]$, the PDF for $A(x)$ and $\psi(x)$ is given by

$$P(A,\psi) = \begin{cases} \frac{A}{2\pi\sigma_x^2} \exp\left(-\frac{A^2}{2\sigma_x^2}\right) & \text{for } A > 0, \quad 0 \le \psi \le 2\pi \\ 0 & \text{otherwise} \end{cases} \qquad (52)$$

Therefore, if we treat the amplitude B and the phase ψ of sinusoidal variation as random variables with PDF given by (52), and take the

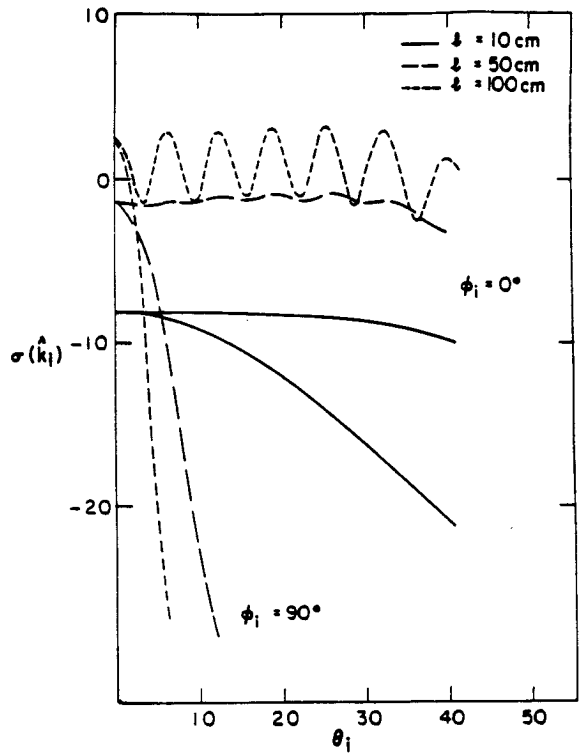

Figure 4.3.11 $\sigma(\hat{k}_i)$ **as a function of** θ_i **for different values of** l **at 1.4 GHz with** $\sigma = 1$ **cm,** $B = 10$ **cm,** $P = 100$ **cm,** $\sigma_x = 5$ **cm,** $l_x = 300$ **cm, and** $\epsilon_1 = (6.0 + i0.6)\epsilon_o$.

average of (51) with respect to B and ψ, we obtain the randomly perturbed quasiperiodic surface result, given by (50), by making use of

$$\int_0^\infty dB\, J_n^2(k_{dz}B)\frac{B}{\sigma_x^2}\exp\left(-\frac{B^2}{2\sigma_x^2}\right) = \exp(-k_{dz}^2\sigma_x^2)I_n(-k_{dz}^2\sigma_x^2) \quad (53)$$

In Figs. 4.3.11 and 4.3.12 we illustrate the combined effect of the previous cases. In Fig. 4.3.11 the backscattering cross sections are plotted for different l for the case $B = 10\,\text{cm}$ and $\sigma_x = 5\,\text{cm}$. The $\phi_i = 0°$ results are seen to be much flatter as a function of incident angle than the corresponding cases in Fig. 4.3.10(a). The effect of varying σ_x is illustrated in Fig. 4.3.12. Therefore, by varying σ_x and B, we can

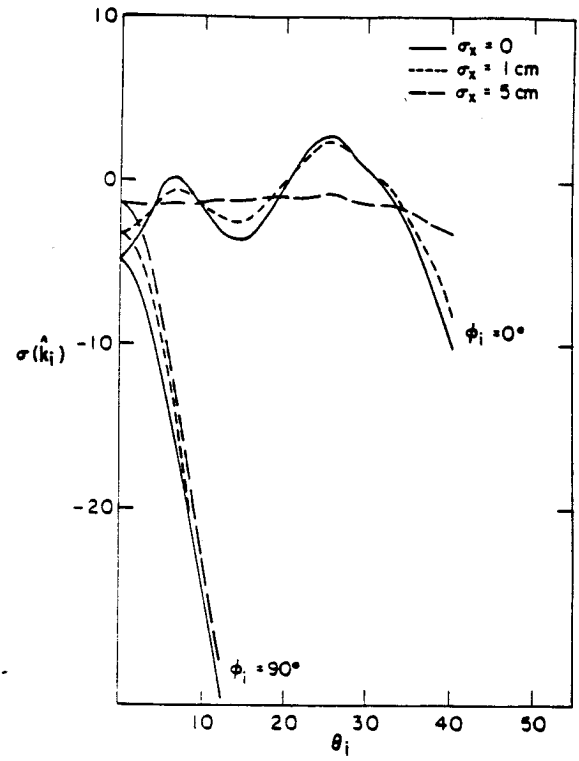

Figure 4.3.12 $\sigma(\hat{k}_i)$ **as a function of** θ_i **for different values of** σ_x **at 1.4 GHz with** $\sigma = 1$ **cm,** $l = 50$ **cm,** $B = 10$ **cm,** $P = 100$ **cm,** $l_x = 300$ **cm, and** $\epsilon_1 = (6.0 + i0.6)\epsilon_o$.

obtain different combinations of the previous two cases when $\sigma_x = 0$ or $B = 0$.

Appendix A. Zeroth-Order Equation and Solution

The zeroth-order equations are given as follows.

$$\hat{h}(-k_{zi}) \cdot \hat{e}_i \delta_m = \sum_{n=-\infty}^{\infty} \frac{k}{2k_{zmi}} Q_{mn}^{-}(k_{zmi}) \left\{ \frac{k_{ymi}}{k_{\rho mi}} \alpha_{xn}^{(0)} \right.$$

$$- \frac{k_{xmi}}{k_{\rho mi}} \alpha_{yn}^{(0)} + \left[\frac{k_{zmi}}{k} \frac{k_{xmi}}{k_{\rho mi}} - \frac{k_{\rho mi}}{k} \frac{(n-m)\frac{2\pi}{p}}{k_{zmi}} \right] \beta_{xn}^{(0)} + \frac{k_{zmi}}{k} \frac{k_{ymi}}{k_{\rho mi}} \beta_{yn}^{(0)} \Bigg\} \tag{A1a}$$

$$\hat{v}(-k_{zi}) \cdot \hat{e}_i \delta_m = \sum_{n=-\infty}^{\infty} \frac{k}{2k_{zmi}} Q_{mn}^{-}(k_{zmi}) \left\{ \left[\frac{k_{zmi}}{k} \frac{k_{xmi}}{k_{\rho mi}} - \frac{k_{\rho mi}}{k} \frac{(n-m)\frac{2\pi}{p}}{k_{zmi}} \right] \alpha_{xn}^{(0)} + \frac{k_{zmi}}{k} \frac{k_{ymi}}{k_{\rho mi}} \alpha_{yn}^{(0)} - \frac{k_{ymi}}{k_{\rho mi}} \beta_{xn}^{(0)} + \frac{k_{xmi}}{k_{\rho mi}} \beta_{yn}^{(0)} \right\} \tag{A1b}$$

$$0 = \sum_{n=-\infty}^{\infty} Q_{mn}^{+}(k_{1zmi}) \left\{ \frac{k}{k_1} \frac{k_{ymi}}{k_{\rho mi}} \alpha_{xn}^{(0)} - \frac{k}{k_1} \frac{k_{xmi}}{k_{\rho mi}} \alpha_{yn}^{(0)} + \left[- \frac{k_{1zmi}}{k_1} \frac{k_{xmi}}{k_{\rho mi}} + \frac{k_{\rho mi}}{k_1} \frac{(n-m)\frac{2\pi}{p}}{k_{1zmi}} \right] \beta_{xn}^{(0)} - \frac{k_{1zmi}}{k_1} \frac{k_{ymi}}{k_{\rho mi}} \beta_{yn}^{(0)} \right\} \tag{A1c}$$

$$0 = \sum_{n=-\infty}^{\infty} Q_{mn}^{+}(k_{1zmi}) \left\{ \frac{k}{k_1} \left[- \frac{k_{1zmi}}{k_1} \frac{k_{xmi}}{k_{\rho mi}} + \frac{k_{\rho mi}}{k_1} \frac{(n-m)\frac{2\pi}{p}}{k_{1zmi}} \right] \alpha_{xn}^{(0)} - \frac{k}{k_1} \frac{k_{1zmi}}{k_1} \frac{k_{ymi}}{k_{\rho mi}} \alpha_{yn}^{(0)} - \frac{k_{ymi}}{k_{\rho mi}} \beta_{xn}^{(0)} + \frac{k_{xmi}}{k_{\rho mi}} \beta_{yn}^{(0)} \right\} \qquad m = -\infty, \ldots, \infty \tag{A1d}$$

where k_{xmi}, k_{ymi}, $k_{\rho mi}$, k_{zmi}, k_{1zmi}, and $Q_{mn}^{\pm}(k_z)$ are given by

$$k_{xmi} = k_{xi} + \frac{2m\pi}{p}, \quad k_{ymi} = k_{yi}, \quad k_{\rho mi} = \sqrt{k_{xmi}^2 + k_{ymi}^2} \tag{A2a}$$

$$k_{zmi} = \sqrt{k^2 - k_{\rho mi}^2}, \quad k_{1zmi} = \sqrt{k_1^2 - k_{\rho mi}^2} \tag{A2b}$$

$$Q_{mn}^{\pm}(k_z) = \frac{1}{p}\int_0^p dx \exp\left[-i(m-n)\frac{2\pi}{p}x \mp ik_z H\cos\left(\frac{2\pi}{p}x\right)\right]$$
$$= (\mp i)^{|m-n|} J_{|m-n|}(k_z H) \tag{A3}$$

The components of the zeroth-order solution are given explicitly as follows.

$$E_{hsm}^{(0)} = \frac{k}{2k_{zmi}}\sum_{n=-\infty}^{\infty} Q_{mn}^{+}(k_{zmi})\left\{-\frac{k_{ymi}}{k_{\rho mi}}\alpha_{xn}^{(0)} + \frac{k_{xmi}}{k_{\rho mi}}\alpha_{yn}^{(0)}\right.$$
$$\left. + \left(\frac{k_{zmi}}{k}\frac{k_{xmi}}{k_{\rho mi}} - \frac{k_{\rho mi}}{k}\frac{(n-m)\frac{2\pi}{p}}{k_{zmi}}\right)\beta_{xn}^{(0)} + \frac{k_{zmi}}{k}\frac{k_{ymi}}{k_{\rho mi}}\beta_{yn}^{(0)}\right\} \tag{A4a}$$

$$E_{vsm}^{(0)} = \frac{k}{2k_{zmi}}\sum_{n=-\infty}^{\infty} Q_{mn}^{+}(k_{zmi})\left\{\left(\frac{k_{zmi}}{k}\frac{k_{xmi}}{k_{\rho mi}} - \frac{k_{\rho mi}}{k}\frac{(n-m)\frac{2\pi}{p}}{k_{zmi}}\right)\alpha_{xn}^{(0)}\right.$$
$$\left. + \frac{k_{zmi}}{k}\frac{k_{ymi}}{k_{\rho mi}}\alpha_{yn}^{(0)} + \frac{k_{ymi}}{k_{\rho mi}}\beta_{xn}^{(0)} - \frac{k_{xmi}}{k_{\rho mi}}\beta_{yn}^{(0)}\right\} \tag{A4b}$$

Appendix B. First-Order Equation and Solution

The first-order equations for the surface fields are given explicitly as follows.

$$\sum_{m=-\infty}^{\infty} Q_{m0}^{-}(k_{zl})\left\{\frac{k_{yl}}{k_{\rho l}}A_x^{(1)}(\bar{k}_{\perp l} - \bar{k}_{\perp mi})\right.$$
$$- \frac{k_{xl}}{k_{\rho l}}A_y^{(1)}(\bar{k}_{\perp l} - \bar{k}_{\perp mi}) + \left(\frac{k_{zl}}{k}\frac{k_{xl}}{k_{\rho l}} + \frac{k_{\rho l}}{k}\frac{m\frac{2\pi}{p}}{k_{zl}}\right)B_x^{(1)}(\bar{k}_{\perp l} - \bar{k}_{\perp mi})$$
$$\left. + \frac{k_{zl}}{k}\frac{k_{yl}}{k_{\rho l}}B_y^{(1)}(\bar{k}_{\perp l} - \bar{k}_{\perp mi})\right\}$$
$$= -\sum_{m=-\infty}^{\infty} ik_{zl}F(\bar{k}_{\perp l} - \bar{k}_{\perp mi})\sum_{n=-\infty}^{\infty} Q_{mn}^{-}(k_{zl})$$
$$\left\{\frac{k_{yl}}{k_{\rho l}}\alpha_{xn}^{(0)} - \frac{k_{xl}}{k_{\rho l}}\alpha_{yn}^{(0)} + \left[\frac{k_{zl}}{k}\frac{k_{xl}}{k_{\rho l}} - \frac{k_{\rho l}}{k}\frac{(n-m)\frac{2\pi}{p}}{k_{zl}}\right.\right.$$

$$+\frac{k_{\rho l}}{k}\frac{(k_{xl}-k_{xmi})}{k_{zl}}\Big]\beta_{xn}^{(0)}+\left[\frac{k_{zl}}{k}\frac{k_{yl}}{k_{\rho l}}+\frac{k_{\rho l}}{k}\frac{(k_{yl}-k_{yi})}{k_{zl}}\right]\beta_{yn}^{(0)}\Bigg\} \tag{B1a}$$

$$\sum_{m=-\infty}^{\infty}Q_{m0}^{-}(k_{zl})\Bigg\{\left(\frac{k_{zl}}{k}\frac{k_{xl}}{k_{\rho l}}+\frac{k_{\rho l}}{k}\frac{m\frac{2\pi}{p}}{k_{zl}}\right)A_x^{(1)}(\overline{k}_{\perp l}-\overline{k}_{\perp mi})$$

$$+\frac{k_{zl}}{k}\frac{k_{yl}}{k_{\rho l}}A_y^{(1)}(\overline{k}_{\perp l}-\overline{k}_{\perp mi})$$

$$-\frac{k_{yl}}{k_{\rho l}}B_x^{(1)}(\overline{k}_{\perp l}-\overline{k}_{\perp mi})+\frac{k_{xl}}{k_{\rho l}}B_y^{(1)}(\overline{k}_{\perp l}-\overline{k}_{\perp mi})\Bigg\}$$

$$=-\sum_{m=-\infty}^{\infty}ik_{zl}F(\overline{k}_{\perp l}-\overline{k}_{\perp mi})\sum_{n=-\infty}^{\infty}Q_{mn}^{-}(k_{zl})$$

$$\Bigg\{\left[\frac{k_{zl}}{k}\frac{k_{xl}}{k_{\rho l}}-\frac{k_{\rho l}}{k}\frac{(n-m)\frac{2\pi}{p}}{k_{zl}}+\frac{k_{\rho l}}{k}\frac{(k_{xl}-k_{xmi})}{k_{zl}}\right]\alpha_{xn}^{(0)}$$

$$+\left[\frac{k_{zl}}{k}\frac{k_{yl}}{k_{\rho l}}+\frac{k_{\rho l}}{k}\frac{(k_{yl}-k_{yi})}{k_{zl}}\right]\alpha_{yn}^{(0)}-\frac{k_{yl}}{k_{\rho l}}\beta_{xn}^{(0)}+\frac{k_{xl}}{k_{\rho l}}\beta_{yn}^{(0)}\Bigg\} \tag{B1b}$$

$$\sum_{m=-\infty}^{\infty}Q_{m0}^{+}(k_{1zl})\Bigg\{\frac{k}{k_1}\frac{k_{yl}}{k_{\rho l}}A_x^{(1)}(\overline{k}_{\perp l}-\overline{k}_{\perp mi})$$

$$-\frac{k}{k_1}\frac{k_{xl}}{k_{\rho l}}A_y^{(1)}(\overline{k}_{\perp l}-\overline{k}_{\perp mi})-\left(\frac{k_{1zl}}{k_1}\frac{k_{xl}}{k_{\rho l}}+\frac{k_{\rho l}}{k_1}\frac{m\frac{2\pi}{p}}{k_{1zl}}\right)$$

$$\times B_x^{(1)}(\overline{k}_{\perp l}-\overline{k}_{\perp mi})-\frac{k_{1zl}}{k_1}\frac{k_{yl}}{k_{\rho l}}B_y^{(1)}(\overline{k}_{\perp l}-\overline{k}_{\perp mi})\Bigg\}$$

$$=-\sum_{m=-\infty}^{\infty}ik_{1zl}F(\overline{k}_{\perp l}-\overline{k}_{\perp mi})\sum_{n=-\infty}^{\infty}Q_{mn}^{+}(k_{1zl})$$

$$\Bigg\{-\frac{k}{k_1}\frac{k_{yl}}{k_{\rho l}}\alpha_{xn}^{(0)}+\frac{k}{k_1}\frac{k_{xl}}{k_{\rho l}}\alpha_{yn}^{(0)}+\left[\frac{k_{1zl}}{k_1}\frac{k_{xl}}{k_{\rho l}}-\frac{k_{\rho l}}{k_1}\frac{(n-m)\frac{2\pi}{p}}{k_{1zl}}\right.$$

$$\left.+\frac{k_{\rho l}}{k_1}\left(\frac{k_{xl}-k_{xmi}}{k_{1zl}}\right)\right]\beta_{xn}^{(0)}+\left[\frac{k_{1zl}}{k_1}\frac{k_{yl}}{k_{\rho l}}+\frac{k_{\rho l}}{k_1}\frac{(k_{yl}-k_{yi})}{k_{1zl}}\right]\beta_{yn}^{(0)}\Bigg\} \tag{B1c}$$

$$\sum_{m=-\infty}^{\infty}Q_{m0}^{+}(k_{1zl})\Bigg\{-\frac{k}{k_1}\left(\frac{k_{1zl}}{k_1}\frac{k_{xl}}{k_{\rho l}}+\frac{k_{\rho l}}{k_1}\frac{m\frac{2\pi}{p}}{k_{1zl}}\right)A_x^{(1)}(\overline{k}_{\perp l}-\overline{k}_{\perp mi})$$

$$
\begin{aligned}
&- \frac{k}{k_1}\frac{k_{1zl}}{k_1}\frac{k_{yl}}{k_{\rho l}} A_y^{(1)}(\bar{k}_{\perp l} - \bar{k}_{\perp mi}) - \frac{k_{yl}}{k_{\rho l}} B_x^{(1)}(\bar{k}_{\perp l} - \bar{k}_{\perp mi}) \\
&+ \frac{k_{xl}}{k_{\rho l}} B_y^{(1)}(\bar{k}_{\perp l} - \bar{k}_{\perp mi}) \Bigg\} \\
&= - \sum_{m=-\infty}^{\infty} ik_{1zl} F(\bar{k}_{\perp l} - \bar{k}_{\perp mi}) \sum_{n=-\infty}^{\infty} Q_{mn}^{+}(k_{1zl}) \\
&\left\{ \frac{k}{k_1} \left[\frac{k_{1zl}}{k_1}\frac{k_{xl}}{k_{\rho l}} - \frac{k_{\rho l}}{k_1}\frac{(n-m)\frac{2\pi}{p}}{k_{1zl}} + \frac{k_{\rho l}}{k_1}\frac{(k_{xl} - k_{xmi})}{k_{1zl}} \right] \alpha_{xn}^{(0)} \right. \\
&+ \frac{k}{k_1} \left[\frac{k_{1zl}}{k_1}\frac{k_{yl}}{k_{\rho l}} + \frac{k_{\rho l}}{k_1}\frac{(k_{yl} - k_{yi})}{k_{1zl}} \right] \alpha_{yn}^{(0)} + \frac{k_{yl}}{k_{\rho l}} \beta_{xn}^{(0)} - \frac{k_{xl}}{k_{\rho l}} \beta_{yn}^{(0)} \Bigg\} \\
&\qquad\qquad l = -\infty, \ldots, \infty \qquad (B1d)
\end{aligned}
$$

where $Q_{mn}^{\pm}$ are given by (A3), and

$$
\bar{k}_{\perp l} = k_{xl}\hat{x} + k_{yl}\hat{y} = \left(k_x + \frac{2l\pi}{p}\right)\hat{x} + k_y\hat{y} \qquad (B2a)
$$

$$
k_{\rho l} = \sqrt{k_{xl}^2 + k_{yl}^2} \qquad (B2b)
$$

$$
k_{zl} = \sqrt{k^2 - k_{\rho l}^2}, \quad k_{1zl} = \sqrt{k_1^2 - k_{\rho l}^2} \qquad (B2c)
$$

The components of the first-order scattered field are given as follows.

$$
\begin{aligned}
E_{hsm}^{(1)} = \frac{k}{2k_z} \Bigg\{ & Q_{m0}^{+}(k_z) \left[-\frac{k_y}{k_\rho} A_x^{(1)}(\bar{k}_\perp - \bar{k}_{\perp mi}) + \frac{k_x}{k_\rho} A_y^{(1)}(\bar{k}_\perp - \bar{k}_{\perp mi}) \right. \\
& \left. + \left(\frac{k_z}{k}\frac{k_x}{k_\rho} + \frac{k_\rho}{k}\frac{m\frac{2\pi}{p}}{k_z}\right) B_x^{(1)}(\bar{k}_\perp - \bar{k}_{\perp mi}) + \frac{k_z}{k}\frac{k_y}{k_\rho} B_y^{(1)}(\bar{k}_\perp - \bar{k}_{\perp mi}) \right] \\
& + ik_z F(\bar{k}_\perp - \bar{k}_{\perp mi}) \sum_{n=-\infty}^{\infty} Q_{mn}^{+}(k_z) \left\{ \frac{k_y}{k_\rho} \alpha_{xn}^{(0)} - \frac{k_x}{k_\rho} \alpha_{yn}^{(0)} \right. \\
& - \left[\frac{k_z}{k}\frac{k_x}{k_\rho} - \frac{k_\rho}{k}\frac{(n-m)\frac{2\pi}{p}}{k_z} + \frac{k_\rho}{k}\frac{(k_x - k_{xmi})}{k_z} \right] \beta_{xn}^{(0)} \\
& \left. - \left[\frac{k_z}{k}\frac{k_y}{k_\rho} + \frac{k_\rho}{k}\frac{(k_y - k_{yi})}{k_z} \right] \beta_{yn}^{(0)} \right\} \Bigg\} \qquad (B3a)
\end{aligned}
$$

$$E_{vsm}^{(1)} = \frac{k}{2k_z}\Bigg\{Q_{m0}^{+}(k_z)\Bigg[\left(\frac{k_z}{k}\frac{k_x}{k_\rho} + \frac{k_\rho}{k}\frac{m\frac{2\pi}{p}}{k_z}\right)A_x^{(1)}(\bar{k}_\perp - \bar{k}_{\perp mi}) + \frac{k_z}{k}\frac{k_y}{k_\rho}A_y^{(1)}(\bar{k}_\perp - \bar{k}_{\perp mi}) + \frac{k_y}{k_\rho}B_x^{(1)}(\bar{k}_\perp - \bar{k}_{\perp mi}) - \frac{k_x}{k_\rho}B_y^{(1)}(\bar{k}_\perp - \bar{k}_{\perp mi})\Bigg] + ik_z F(\bar{k}_\perp - \bar{k}_{\perp mi})\sum_{n=-\infty}^{\infty} Q_{mn}^{+}(k_z)\Bigg\{-\Bigg[\frac{k_z}{k}\frac{k_x}{k_\rho} - \frac{k_\rho}{k}\frac{(n-m)\frac{2\pi}{p}}{k_z} + \frac{k_\rho}{k}\frac{(k_x - k_{xmi})}{k_z}\Bigg]\alpha_{xn}^{(0)} - \left[\frac{k_z}{k}\frac{k_y}{k_\rho} + \frac{k_\rho}{k}\frac{(k_y - k_{yi})}{k_z}\right]\alpha_{yn}^{(0)} - \frac{k_y}{k_\rho}\beta_{xn}^{(0)} + \frac{k_x}{k_\rho}\beta_{yn}^{(0)}\Bigg\}\Bigg\} \qquad (B3b)$$

Appendix C. Second-Order Equation and Solution

The second-order equations are given as follows.

$$\sum_{m=-\infty}^{\infty}\frac{1}{2}Q_{m0}^{-}(k_{zl})\Bigg\{\frac{k_{yl}}{k_{\rho l}}A_x^{(2)}(\bar{k}_{\perp l} - \bar{k}_{\perp mi}) - \frac{k_{xl}}{k_{\rho l}}A_y^{(2)}(\bar{k}_{\perp l} - \bar{k}_{\perp mi}) + \left(\frac{k_{zl}}{k}\frac{k_{xl}}{k_{\rho l}} + \frac{k_{\rho l}}{k}\frac{m\frac{2\pi}{p}}{k_{zl}}\right)B_x^{(2)}(\bar{k}_{\perp l} - \bar{k}_{\perp mi}) + \frac{k_{zl}}{k}\frac{k_{yl}}{k_{\rho l}}B_y^{(2)}(\bar{k}_{\perp l} - \bar{k}_{\perp mi})\Bigg\}$$

$$= -\sum_{m=-\infty}^{\infty}F * F(\bar{k}_{\perp l} - \bar{k}_{\perp mi})\sum_{n=-\infty}^{\infty}Q_{mn}^{-}(k_{zl})\left(-\frac{1}{2}\right)k_{zl}^2 \Bigg\{\frac{k_{yl}}{k_{\rho l}}\alpha_{xn}^{(0)} - \frac{k_{xl}}{k_{\rho l}}\alpha_{yn}^{(0)} + \Bigg[\frac{k_{zl}}{k}\frac{k_{xl}}{k_{\rho l}} - \frac{k_{\rho l}}{k}\frac{(n-m)\frac{2\pi}{p}}{k_{zl}} + \frac{k_{\rho l}}{k}\frac{(k_{xl} - k_{xmi})}{k_{zl}}\Bigg]\beta_{xn}^{(0)} + \left[\frac{k_{zl}}{k}\frac{k_{yl}}{k_{\rho l}} + \frac{k_{\rho l}}{k}\frac{(k_{yl} - k_{yi})}{k_{zl}}\right]\beta_{yn}^{(0)}\Bigg\}$$

$$-\sum_{m=-\infty}^{\infty}ik_{zl}Q_{m0}^{-}(k_{zl})\Bigg\{\frac{k_{yl}}{k_{\rho l}}F * A_x^{(1)}(\bar{k}_{\perp l} - \bar{k}_{\perp mi})$$

$$
\begin{aligned}
&- \frac{k_{xl}}{k_{\rho l}} F * A_y^{(1)}(\bar{k}_{\perp l} - \bar{k}_{\perp mi}) \\
&+ \left(\frac{k_{zl}}{k} \frac{k_{xl}}{k_{\rho l}} + \frac{k_{\rho l}}{k} \frac{m\frac{2\pi}{p}}{k_{zl}} \right) F * B_x^{(1)}(\bar{k}_{\perp l} - \bar{k}_{\perp mi}) \\
&+ \frac{k_{zl}}{k} \frac{k_{yl}}{k_{\rho l}} F * B_y^{(1)}(\bar{k}_{\perp l} - \bar{k}_{\perp mi}) \\
&+ \frac{k_{\rho l}}{k k_{zl}} [(k_{xl} - k_{xmi}) F(\bar{k}_{\perp l} - \bar{k}_{\perp mi})] * B_x^{(1)}(\bar{k}_{\perp l} - \bar{k}_{\perp mi}) \\
&+ \frac{k_{\rho l}}{k k_{zl}} [(k_{yl} - k_{ymi}) F(\bar{k}_{\perp l} - \bar{k}_{\perp mi})] * B_y^{(1)}(\bar{k}_{\perp l} - \bar{k}_{\perp mi}) \Bigg\} \qquad (C1a)
\end{aligned}
$$

$$
\begin{aligned}
&\sum_{m=-\infty}^{\infty} \frac{1}{2} Q_{m0}^{-}(k_{zl}) \Bigg\{ \left(\frac{k_{zl}}{k} \frac{k_{xl}}{k_{\rho l}} + \frac{k_{\rho l}}{k} \frac{m\frac{2\pi}{p}}{k_{zl}} \right) A_x^{(2)}(\bar{k}_{\perp l} - \bar{k}_{\perp mi}) \\
&+ \frac{k_{zl}}{k} \frac{k_{yl}}{k_{\rho l}} A_y^{(2)}(\bar{k}_{\perp l} - \bar{k}_{\perp mi}) - \frac{k_{yl}}{k_{\rho l}} B_x^{(2)}(\bar{k}_{\perp l} - \bar{k}_{\perp mi}) \\
&+ \frac{k_{xl}}{k_{\rho l}} B_y^{(2)}(\bar{k}_{\perp l} - \bar{k}_{\perp mi}) \Bigg\} \\
&= - \sum_{m=-\infty}^{\infty} F * F(\bar{k}_{\perp l} - \bar{k}_{\perp mi}) \sum_{n=-\infty}^{\infty} Q_{mn}^{-}(k_{zl}) \left(-\frac{1}{2} \right) k_{zl}^2 \\
&\Bigg\{ \left[\frac{k_{zl}}{k} \frac{k_{xl}}{k_{\rho l}} - \frac{k_{\rho l}}{k} \frac{(n-m)\frac{2\pi}{p}}{k_{zl}} + \frac{k_{\rho l}}{k} \frac{(k_{xl} - k_{xmi})}{k_{zl}} \right] \alpha_{xn}^{(0)} \\
&+ \left[\frac{k_{zl}}{k} \frac{k_{yl}}{k_{\rho l}} + \frac{k_{\rho l}}{k} \frac{(k_{yl} - k_{yi})}{k_{zl}} \right] \alpha_{yn}^{(0)} - \frac{k_{yl}}{k_{\rho l}} \beta_{xn}^{(0)} + \frac{k_{xl}}{k_{\rho l}} \beta_{yn}^{(0)} \Bigg\} \\
&- \sum_{m=-\infty}^{\infty} i k_{zl} Q_{m0}^{-}(k_{zl}) \Bigg\{ \left(\frac{k_{zl}}{k} \frac{k_{xl}}{k_{\rho l}} + \frac{k_{\rho l}}{k} \frac{m\frac{2\pi}{p}}{k_{zl}} \right) F * A_x^{(1)}(\bar{k}_{\perp l} - \bar{k}_{\perp mi}) \\
&+ \frac{k_{zl}}{k} \frac{k_{yl}}{k_{\rho l}} F * A_y^{(1)}(\bar{k}_{\perp l} - \bar{k}_{\perp mi}) \\
&- \frac{k_{yl}}{k_{\rho l}} F * B_x^{(1)}(\bar{k}_{\perp l} - \bar{k}_{\perp mi}) + \frac{k_{xl}}{k_{\rho l}} F * B_y^{(1)}(\bar{k}_{\perp l} - \bar{k}_{\perp mi}) \\
&+ \frac{k_{\rho l}}{k k_{zl}} [(k_{xl} - k_{xmi}) F(\bar{k}_{\perp l} - \bar{k}_{\perp mi})] * A_x^{(1)}(\bar{k}_{\perp l} - \bar{k}_{\perp mi})
\end{aligned}
$$

$$+\frac{k_{\rho l}}{kk_{zl}}[(k_{yl}-k_{ymi})F(\overline{k}_{\perp l}-\overline{k}_{\perp mi})]*A_y^{(1)}(\overline{k}_{\perp l}-\overline{k}_{\perp mi})\Bigg\} \qquad (C1b)$$

$$\sum_{m=-\infty}^{\infty}\frac{1}{2}Q_{m0}^{+}(k_{1zl})\Bigg\{\frac{k}{k_1}\frac{k_{yl}}{k_{\rho l}}A_x^{(2)}(\overline{k}_{\perp l}-\overline{k}_{\perp mi})$$

$$-\frac{k}{k_1}\frac{k_{xl}}{k_{\rho l}}A_y^{(2)}(\overline{k}_{\perp l}-\overline{k}_{\perp mi})$$

$$-\left(\frac{k_{1zl}}{k_1}\frac{k_{xl}}{k_{\rho l}}+\frac{k_{\rho l}}{k_1}\frac{m\frac{2\pi}{p}}{k_{1zl}}\right)B_x^{(2)}(\overline{k}_{\perp l}-\overline{k}_{\perp mi})$$

$$-\frac{k_{1zl}}{k_1}\frac{k_{yl}}{k_{\rho l}}B_y^{(2)}(\overline{k}_{\perp l}-\overline{k}_{\perp mi})\Bigg\}$$

$$=-\sum_{m=-\infty}^{\infty}F*F(\overline{k}_{\perp l}-\overline{k}_{\perp mi})\sum_{n=-\infty}^{\infty}Q_{mn}^{+}(k_{1zl})(-\frac{1}{2})k_{1zl}^2$$

$$\Bigg\{\frac{k}{k_1}\frac{k_{yl}}{k_{\rho l}}\alpha_{xn}^{(0)}-\frac{k}{k_1}\frac{k_{xl}}{k_{\rho l}}\alpha_{yn}^{(0)}-\left[\frac{k_{1zl}}{k_1}\frac{k_{xl}}{k_{\rho l}}-\frac{k_{\rho l}}{k_1}\frac{(n-m)\frac{2\pi}{p}}{k_{1zl}}\right.$$

$$\left.+\frac{k_{\rho l}}{k_1}\frac{(k_{xl}-k_{xmi})}{k_{1zl}}\right]\beta_{xn}^{(0)}-\left[\frac{k_{1zl}}{k_1}\frac{k_{yl}}{k_{\rho l}}+\frac{k_{\rho l}}{k_1}\frac{(k_{yl}-k_{yi})}{k_{1zl}}\right]\beta_{yn}^{(0)}\Bigg\}$$

$$-\sum_{m=-\infty}^{\infty}-ik_{1zl}Q_{m0}^{+}(k_{1zl})\Bigg\{\frac{k}{k_1}\frac{k_{yl}}{k_{\rho l}}F*A_x^{(1)}(\overline{k}_{\perp l}-\overline{k}_{\perp mi})$$

$$-\frac{k}{k_1}\frac{k_{xl}}{k_{\rho l}}F*A_y^{(1)}(\overline{k}_{\perp l}-\overline{k}_{\perp mi})$$

$$-\left(\frac{k_{1zl}}{k_1}\frac{k_{xl}}{k_{\rho l}}+\frac{k_{\rho l}}{k_1}\frac{m\frac{2\pi}{p}}{k_{1zl}}\right)F*B_x^{(1)}(\overline{k}_{\perp l}-\overline{k}_{\perp mi})$$

$$-\frac{k_{1zl}}{k_1}\frac{k_{yl}}{k_{\rho l}}F*B_y^{(1)}(\overline{k}_{\perp l}-\overline{k}_{\perp mi})$$

$$-\frac{k_{\rho l}}{k_1k_{1zl}}[(k_{xl}-k_{xmi})F(\overline{k}_{\perp l}-\overline{k}_{\perp mi})]*B_x^{(1)}(\overline{k}_{\perp l}-\overline{k}_{\perp mi})$$

$$-\frac{k_{\rho l}}{k_1k_{1zl}}[(k_{yl}-k_{ymi})F(\overline{k}_{\perp l}-\overline{k}_{\perp mi})]*B_y^{(1)}(\overline{k}_{\perp l}-\overline{k}_{\perp mi})\Bigg\}$$

$$(C1c)$$

$$\sum_{m=-\infty}^{\infty}\frac{1}{2}Q_{m0}^{+}(k_{1zl})\left\{-\frac{k}{k_1}\left(\frac{k_{1zl}}{k_1}\frac{k_{xl}}{k_{\rho l}}+\frac{k_{\rho l}}{k_1}\frac{m\frac{2\pi}{p}}{k_{1zl}}\right)A_x^{(2)}(\bar{k}_{\perp l}-\bar{k}_{\perp mi})\right.$$
$$-\frac{k}{k_1}\frac{k_{1zl}}{k_1}\frac{k_{yl}}{k_{\rho l}}A_y^{(2)}(\bar{k}_{\perp l}-\bar{k}_{\perp mi})-\frac{k_{yl}}{k_{\rho l}}B_x^{(2)}(\bar{k}_{\perp l}-\bar{k}_{\perp mi})$$
$$\left.+\frac{k_{xl}}{k_{\rho l}}B_y^{(2)}(\bar{k}_{\perp l}-\bar{k}_{\perp mi})\right\}$$
$$=-\sum_{m=-\infty}^{\infty}F*F(\bar{k}_{\perp l}-\bar{k}_{\perp mi})\sum_{n=-\infty}^{\infty}Q_{mn}^{+}(k_{1zl})\left(-\frac{1}{2}\right)k_{1zl}^2$$
$$\left\{-\frac{k}{k_1}\left[\frac{k_{1zl}}{k_1}\frac{k_{xl}}{k_{\rho l}}-\frac{k_{\rho l}}{k_1}\frac{(n-m)\frac{2\pi}{p}}{k_{1zl}}+\frac{k_{\rho l}}{k_1}\frac{(k_{xl}-k_{xmi})}{k_{1zl}}\right]\alpha_{xn}^{(0)}\right.$$
$$\left.-\frac{k}{k_1}\left[\frac{k_{1zl}}{k_1}\frac{k_{yl}}{k_{\rho l}}+\frac{k_{\rho l}}{k_1}\frac{(k_{yl}-k_{yi})}{k_{1zl}}\right]\alpha_{yn}^{(0)}-\frac{k_{yl}}{k_{\rho l}}\beta_{xn}^{(0)}+\frac{k_{xl}}{k_{\rho l}}\beta_{yn}^{(0)}\right\}$$
$$-\sum_{m=-\infty}^{\infty}-ik_{1zl}Q_{m0}^{+}(k_{1zl})\left\{-\frac{k}{k_1}\left(\frac{k_{1zl}}{k_1}\frac{k_{xl}}{k_{\rho l}}\right.\right.$$
$$\left.+\frac{k_{\rho l}}{k_1}\frac{m\frac{2\pi}{p}}{k_{1zl}}\right)F*A_x^{(1)}(\bar{k}_{\perp l}-\bar{k}_{\perp mi})$$
$$-\frac{k}{k_1}\frac{k_{1zl}}{k_1}\frac{k_{yl}}{k_{\rho l}}F*A_y^{(1)}(\bar{k}_{\perp l}-\bar{k}_{\perp mi})-\frac{k_{yl}}{k_{\rho l}}F*B_x^{(1)}(\bar{k}_{\perp l}-\bar{k}_{\perp mi})$$
$$+\frac{k_{xl}}{k_{\rho l}}F*B_y^{(1)}(\bar{k}_{\perp l}-\bar{k}_{\perp mi})$$
$$-\frac{k}{k_1}\frac{k_{\rho l}}{k_1k_{1zl}}[(k_{xl}-k_{xmi})F(\bar{k}_{\perp l}-\bar{k}_{\perp mi})]*A_x^{(1)}(\bar{k}_{\perp l}-\bar{k}_{\perp mi})$$
$$\left.-\frac{k}{k_1}\frac{k_{\rho l}}{k_1k_{1zl}}[(k_{yl}-k_{ymi})F(\bar{k}_{\perp l}-\bar{k}_{\perp mi})]*A_y^{(1)}(\bar{k}_{\perp l}-\bar{k}_{\perp mi})\right\} \tag{C1d}$$

where $Q_{mn}^{\pm}$ are given by (A3).

The components of the second-order scattered field are given explicitly below.

$$E_{hsm}^{(2)}=\left(-\frac{k}{2k_z}\right)\left\{\sum_{m=-\infty}^{\infty}\frac{1}{2}Q_{m0}^{+}(k_z)\left[\frac{k_y}{k_\rho}A_x^{(2)}(\bar{k}_{\perp}-\bar{k}_{\perp mi})\right.\right.$$

$$
\begin{aligned}
&- \frac{k_x}{k_\rho} A_y^{(2)}(\bar{k}_\perp - \bar{k}_{\perp mi}) - \frac{k_z}{k}\frac{k_y}{k_\rho} B_y^{(2)}(\bar{k}_\perp - \bar{k}_{\perp mi}) \\
&- \left(\frac{k_z}{k}\frac{k_x}{k_\rho} + \frac{k_\rho}{k}\frac{m\frac{2\pi}{p}}{k_z}\right) B_x^{(2)}(\bar{k}_\perp - \bar{k}_{\perp mi})\Bigg] \\
&+ \sum_{m=-\infty}^{\infty} F * F(\bar{k}_\perp - \bar{k}_{\perp mi}) \sum_{n=-\infty}^{\infty} Q_{mn}^{+}(k_z) \left(-\frac{1}{2}\right) k_z^2 \Bigg[\frac{k_y}{k_\rho}\alpha_{xn}^{(0)} \\
&- \frac{k_x}{k_\rho}\alpha_{yn}^{(0)} - \left[\frac{k_z}{k}\frac{k_x}{k_\rho} - \frac{k_\rho}{k}\frac{(n-m)\frac{2\pi}{p}}{k_z} + \frac{k_\rho}{k}\frac{(k_x - k_{xmi})}{k_z}\right]\beta_{xn}^{(0)} \\
&- \left[\frac{k_z}{k}\frac{k_y}{k_\rho} + \frac{k_\rho}{k}\frac{(k_y - k_{yi})}{k_z}\right]\beta_{yn}^{(0)}\Bigg] \\
&- \sum_{m=-\infty}^{\infty} ik_z Q_{m0}^{+}(k_z)\Bigg[\frac{k_y}{k_\rho} F * A_x^{(1)}(\bar{k}_\perp - \bar{k}_{\perp mi}) \\
&- \frac{k_x}{k_\rho} F * A_y^{(1)}(\bar{k}_\perp - \bar{k}_{\perp mi}) \\
&- \left(\frac{k_z}{k}\frac{k_x}{k_\rho} + \frac{k_\rho}{k}\frac{m\frac{2\pi}{p}}{k_z}\right) F * B_x^{(1)}(\bar{k}_\perp - \bar{k}_{\perp mi}) \\
&- \frac{k_z}{k}\frac{k_y}{k_\rho} F * B_y^{(1)}(\bar{k}_\perp - \bar{k}_{\perp mi}) \\
&- \frac{k_\rho}{k k_z}[(k_x - k_{xmi}) F(\bar{k}_\perp - \bar{k}_{\perp mi})] * B_x^{(1)}(\bar{k}_\perp - \bar{k}_{\perp mi}) \\
&- \frac{k_\rho}{k k_z}[(k_y - k_{ymi}) F(\bar{k}_\perp - \bar{k}_{\perp mi})] * B_y^{(1)}(\bar{k}_\perp - \bar{k}_{\perp mi})\Bigg]\Bigg\} \qquad (C2a)
\end{aligned}
$$

$$
\begin{aligned}
E_{vsm}^{(2)} = &\left(-\frac{k}{2k_z}\right)\Bigg\{\sum_{m=-\infty}^{\infty} \frac{1}{2} Q_{m0}^{+}(k_z)\Bigg[-\Bigg(\frac{k_z}{k}\frac{k_x}{k_\rho} \\
&+ \frac{k_\rho}{k}\frac{m\frac{2\pi}{p}}{k_z}\Bigg) A_x^{(2)}(\bar{k}_\perp - \bar{k}_{\perp mi}) - \frac{k_z}{k}\frac{k_y}{k_\rho} A_y^{(2)}(\bar{k}_\perp - \bar{k}_{\perp mi}) \\
&- \frac{k_y}{k_\rho} B_x^{(2)}(\bar{k}_\perp - \bar{k}_{\perp mi}) + \frac{k_x}{k_\rho} B_y^{(2)}(\bar{k}_\perp - \bar{k}_{\perp mi})\Bigg] \\
&+ \sum_{m=-\infty}^{\infty} F * F(\bar{k}_\perp - \bar{k}_{\perp mi}) \sum_{n=-\infty}^{\infty} Q_{mn}^{+}(k_z) \left(-\frac{1}{2}\right) k_z^2
\end{aligned}
$$

$$\left[-\left[\frac{k_z}{k}\frac{k_x}{k_\rho}-\frac{k_\rho}{k}\frac{(n-m)\frac{2\pi}{p}}{k_z}+\frac{k_\rho}{k}\frac{(k_x-k_{xmi})}{k_z}\right]\alpha_{xn}^{(0)}\right.$$
$$-\left[\frac{k_z}{k}\frac{k_y}{k_\rho}+\frac{k_\rho}{k}\frac{(k_y-k_{yi})}{k_z}\right]\alpha_{yn}^{(0)}-\frac{k_y}{k_\rho}\beta_{xn}^{(0)}+\frac{k_x}{k_\rho}\beta_{yn}^{(0)}\Bigg]$$
$$-\sum_{m=-\infty}^{\infty} ik_z Q_{m0}^{+}(k_z)\left[-\left(\frac{k_z}{k}\frac{k_x}{k_\rho}+\frac{k_\rho}{k}\frac{m\frac{2\pi}{p}}{k_z}\right)F*A_x^{(1)}(\bar{k}_\perp-\bar{k}_{\perp mi})\right.$$
$$-\frac{k_z}{k}\frac{k_y}{k_\rho}F*A_y^{(1)}(\bar{k}_\perp-\bar{k}_{\perp mi})$$
$$-\frac{k_y}{k_\rho}F*B_x^{(1)}(\bar{k}_\perp-\bar{k}_{\perp mi})+\frac{k_x}{k_\rho}F*B_y^{(1)}(\bar{k}_\perp-\bar{k}_{\perp mi})$$
$$-\frac{k_\rho}{kk_z}[(k_x-k_{xmi})F(\bar{k}_\perp-\bar{k}_{\perp mi})]*A_x^{(1)}(\bar{k}_\perp-\bar{k}_{\perp mi})$$
$$\left.\left.-\frac{k_\rho}{kk_z}[(k_y-k_{ymi})F(\bar{k}_\perp-\bar{k}_{\perp mi})]*A_y^{(1)}(\bar{k}_\perp-\bar{k}_{\perp mi})\right]\right\} \qquad (C2b)$$

Appendix D. Narrow-Band Gaussian Random Process

The narrow-band Gaussian random process can be expressed as [Davenport and Root, 1958]

$$A(x)\cos\left[\frac{2\pi}{P}x+\psi(x)\right]=\xi_c(x)\cos\frac{2\pi}{P}x-\xi_s\sin\frac{2\pi}{P}x \qquad (D1)$$

where $\xi_c(x)$ and $\xi_s(x)$ are independent Gaussian

$$\langle\xi_c(x)\rangle=\langle\xi_s(x)\rangle=0 \qquad (D2)$$

and

$$\langle\xi_c(x_1)\xi_c(x_2)\rangle=\langle\xi_s(x_1)\xi_s(x_2)\rangle=\sigma_x^2 C_x(|x_1-x_2|) \qquad (D3)$$
$$\langle\xi_c(x_1)\xi_s(x_2)\rangle=0 \qquad (D4)$$

where σ_x is the standard deviation of $\xi_c(x)$ and $\xi_s(x)$ and $C_x(|x_1-x_2|)$ is the normalized correlation function. The covariance of narrow-band Gaussian random processes at x_1 and x_2 is given by

$$\left\langle A(x_1)\cos\left[\frac{2\pi}{P}x_1+\psi(x_1)\right]A(x_2)\cos\left[\frac{2\pi}{P}x_2+\psi(x_2)\right]\right\rangle$$
$$=\sigma_x^2 C_x(|x_1-x_2|)\cos\frac{2\pi}{P}(x_1-x_2) \qquad (D5)$$

The probability density function in terms of A and ψ is given by

$$P(A,\psi) = \begin{cases} \frac{A}{2\pi\sigma_s^2} \exp\left(-\frac{A^2}{2\sigma_s^2}\right) & \text{for } A > 0, \quad 0 \le \psi \le 2\pi \\ 0 & \text{otherwise} \end{cases} \tag{D6}$$

Appendix E. Calculations of $|\langle I\rangle|^2$ and D_I

The integral I is given by

$$I = \int_{A_o} \exp(i\bar{k}_d \cdot \bar{r}')d\bar{r}'_\perp \tag{E1}$$

The ensemble average of I is given by

$$\langle I\rangle = \int_{A_o} dx'dy' \exp(ik_{dx}x' + ik_{dy}y')\langle \exp[ik_{dz}f(x',y')]\rangle \tag{E2}$$

with

$$\begin{aligned} \langle \exp[ik_{dz}f(x',y')]\rangle = &\exp\left[-\frac{1}{2}k_{dz}^2(\sigma^2+\sigma_x^2)\right] \\ &\times \exp\left[ik_{dz}B\cos\left(\frac{2\pi}{P}x' + \phi\right)\right] \end{aligned} \tag{E3}$$

$$\sigma^2 = \langle \xi^2\rangle \tag{E4}$$

$$\sigma_x^2 = \langle \xi_c^2\rangle = \langle \xi_s^2\rangle \tag{E5}$$

Therefore,

$$\begin{aligned} \langle I\rangle = &4L_xL_y \exp\left[-\frac{1}{2}k_{dz}^2(\sigma^2+\sigma_x^2)\right] \sum_{n=-\infty}^{\infty} a_n \\ &\times \operatorname{sinc}\left[\left(k_{dz} + n\frac{2\pi}{P}\right)L_x\right] \operatorname{sinc}[k_{dy}L_y] \end{aligned} \tag{E6}$$

where

$$a_n = (-1)^n J_n(-k_{dz}B)\exp\left[in\left(\frac{\pi}{2}+\phi\right)\right] \tag{E7}$$

J_n is the nth-order Bessel function, and $2L_x$ and $2L_y$ are the lengths of the rough surface in the x and y directions, respectively, so that

$$A_o = 4L_xL_y \tag{E8}$$

Assuming that the area illuminated contains many periods ($L_x, L_y \gg P$), we have

$$|\langle I\rangle|^2 \simeq 16L_x^2L_y^2 \exp\left[-k_{dz}^2(\sigma^2+\sigma_x^2)\right] \sum_{n=-\infty}^{\infty} |a_n|^2 \times \operatorname{sinc}^2\left[\left(k_{dz}+n\frac{2\pi}{P}\right)L_x\right] \operatorname{sinc}^2\left[k_{dy}L_y\right] \tag{E9}$$

By allowing L_x and L_y to approach infinity in the above equation, we obtain

$$|\langle I\rangle|^2 = 4\pi^2 A_o \exp\left[-k_{dz}^2(\sigma^2+\sigma_x^2)\right] \sum_{n=-\infty}^{\infty} |a_n|^2 \delta\left(k_{dx}+n\frac{2\pi}{P}\right)\delta\left(k_{dy}\right) \tag{E10}$$

where δ is the Dirac delta function.

$$\langle II^*\rangle = \int_{A_o} d\bar{r}_\perp \int_{A_O} d\bar{r}'_\perp \exp\left[i\bar{k}_{d\perp}\cdot(\bar{r}_\perp-\bar{r}'_\perp\right] \langle \exp\left(i\bar{k}_{dz}[f(x,y)-f(x',y')]\right)\rangle \tag{E11}$$

With the change of variables we have

$$\begin{aligned}\langle II^*\rangle = \frac{1}{4}\int_{-2L_x+|x|}^{2L_x-|x|} dx' \int_{-2L_y+|y|}^{2L_y-|y|} dy' \int_{-2L_x}^{2L_x} dx \int_{-2L_y}^{2L_y} dy \\ \times \exp\left[i\bar{k}_{d\perp}\cdot\bar{r}_\perp\right] \sum_{n=-\infty}^{\infty} a_n(x)\exp\left[i\frac{n}{2}\frac{2\pi}{P}x'\right] \\ \times \exp\left[-k_{dz}^2\sigma^2+k_{dz}^2\sigma^2C(\bar{r}_\perp)\right] \\ \times \exp\left[-k_{dz}^2\sigma_x^2+k_{dz}^2\sigma_x^2\cos\frac{2\pi}{P}x\,C_x(x)\right]\end{aligned} \tag{E12}$$

where

$$a_n(x) = J_n\left[2k_{dz}B\sin\left(\frac{\pi}{P}x\right)\right]$$

Expanding $a_n(x)$ and carrying out the dx' and dy' integrations, we obtain

$$\langle II^*\rangle = \frac{1}{2}\int_{-2L_x}^{2L_x} dx \int_{-2L_y}^{2L_y} dy \sum_{n=-\infty}^{\infty}\sum_{\mu=-\infty}^{\infty} \beta_{n\mu}\exp\left[i\left(\bar{k}_{d\perp}+\hat{x}\mu\frac{2\pi}{P}\right)\cdot\bar{r}_\perp\right]$$

$$[2L_y - |y|]\frac{1}{in\frac{2\pi}{P}}\left\{\exp\left[in\frac{2\pi}{P}(2L_x - |x|)\right]\right.$$
$$\left. - \exp\left[-in\frac{2\pi}{P}(2L_x - |x|)\right]\right\}\exp\left[-k_{dz}^2\sigma^2 + k_{dz}^2\sigma^2 C(\bar{r}_\perp)\right]$$
$$\times \exp\left[-k_{dz}^2\sigma_x^2 + k_{dz}^2\sigma_x^2\cos\frac{2\pi}{P}x\, C_x(x)\right] \qquad (E13)$$

where

$$\beta_{n\mu} = (-1)^\mu J_{n-\mu}(k_{dz}B)\, J_{n+\mu}(k_{dz}B)$$

It is clear from the above equation that the $n = 0$ term is proportional to L_x, while the $n \neq 0$ term is proportional to P. The argument of the Bessel function $k_{dz}B$ will dictate the number of terms that needs to be summed up. However, if $L_x \gg P$ (we eventually take the limit $L_x \to \infty$ later on), then the $n = 0$ term will make dominant contributions, and other terms will be negligible. Therefore, keeping only the $n = 0$ term, we obtain

$$\langle II^*\rangle = \int_{-2L_x}^{2L_x} dx \int_{-2L_y}^{2L_y} dy \sum_{\mu=-\infty}^{\infty} b_\mu \exp\left[i\left(\bar{k}_{d\perp} + \hat{x}\mu\frac{2\pi}{P}\right)\cdot\bar{r}_\perp\right]$$
$$[2L_x - |x|][2L_y - |y|]\exp\left[-k_{dz}^2\sigma^2 + k_{dz}^2\sigma^2 C(\bar{r}_\perp)\right]$$
$$\times \exp\left[-k_{dz}^2\sigma_x^2 + k_{dz}^2\sigma_x^2\cos\frac{2\pi}{P}x\, C_x(x)\right] \qquad (E14)$$

where

$$b_\mu = J_\mu^2(k_{dz}B) \qquad (E15)$$

We assume the correlation functions $C(\bar{r}_\perp)$ and $C_x(x)$ to have a Gaussian form

$$C(\bar{r}_\perp) = \exp\left[-(x^2 + y^2)/l^2\right] \qquad (E16)$$
$$C_x(x) = \exp\left[-x^2/l_x^2\right] \qquad (E17)$$

where l is the correlation length for the random variable $\xi(\bar{r}\ \perp)$ in the transverse plane, and l_x is the correlation length for the random variables $\xi_c(x)$ and $\xi_s(x)$ in the x direction.

The expressions for the standard deviation of the integral I can now be evaluated in a closed form. Assuming $L_x, L_y \gg l, l_x, P$, we obtain from $(E10), (E14), (E16)$, and $(E17)$,

$$D_I = \langle II^*\rangle - |\langle I\rangle| = \frac{4\pi A_o}{k^2}(D_{I_1} + D_{I_2}) \qquad (E18)$$

with

$$D_{I_1} = \frac{k^2}{4} \sum_{\mu=-\infty}^{\infty} b_\mu \exp\left[-k_{dz}^2(\sigma^2+\sigma_x^2)\right] \sum_{m=1}^{\infty} \frac{(k_{dz}^2\sigma^2)^m}{m!}$$
$$\times \frac{l^2}{m}\left(\exp\left\{-\left[\left(k_{dx}+\mu\frac{2\pi}{P}\right)^2+k_{dy}^2\right]\frac{l^2}{4m}\right\}\right.$$
$$+\sum_{m'=1}^{\infty}\sum_{n=0}^{m'}\frac{1}{2^{m'}}\binom{m'}{n}\frac{(k_{dz}^2\sigma_x^2)^{m'}}{m'!}$$
$$\left.\times\frac{1}{q}\exp\left\{-k_{dy}^2\frac{l^2}{4m}-\left[k_{dx}+(\mu+m'-2n)\frac{2\pi}{P}\right]^2\frac{l^2}{4mq}\right\}\right) \tag{E19}$$

where

$$q=\sqrt{1+\frac{l^2m'}{l_x^2m}}$$

and

$$D_{I_2} = \frac{k^2}{2}\delta(k_{dy})\sum_{\mu=-\infty}^{\infty} b_\mu \sum_{m=1}^{\infty}\sum_{n=0}^{m}\frac{1}{2^m}\binom{m}{n}\exp\left[-k_{dz}^2(\sigma^2+\sigma_x^2)\right]$$
$$\times\sqrt{\frac{\pi}{m}}\,l_x\frac{(k_{dz}^2\sigma_x^2)^m}{m!}\exp\left\{-\left[k_{dx}+(\mu+m-2n)\frac{2\pi}{P}\right]^2\frac{l_x^2}{4m}\right\} \tag{E20}$$

where we made use of

$$\lim_{L_y\to\infty}\frac{L_y}{\pi}\mathrm{sinc}^2\left(k_{dy}L_y\right)=\delta(k_{dy}) \tag{E21}$$

We note that when $l \gg l_x, P$, the expressions for D_{I_1}, (E19), can be simplified to

$$D_{I_1} \simeq \frac{k^2}{4}\sum_{\mu=-\infty}^{\infty} b_\mu \exp\left[-k_{dz}^2(\sigma^2+\sigma_x^2)\right]\sum_{m=1}^{\infty}\frac{(k_{dz}^2\sigma^2)^m}{m!}\frac{l^2}{m}$$
$$\exp\left\{-\left[\left(k_{dx}+\mu\frac{2\pi}{P}\right)^2+k_{dy}^2\right]\frac{l^2}{4m}\right\} \tag{E22}$$

After some manipulations, the above expression further simplifies to

$$D_{I_1} \simeq \frac{1}{P}\int_0^P dx\,\frac{k^2}{4}\exp\left[-k_{dz}^2(\sigma^2+\sigma_x^2)\right]\sum_{m=1}^{\infty}\frac{(k_{dz}^2\sigma^2)^m}{m!}\frac{l^2}{m}$$
$$\times\exp\left\{-\left[\left(k_{dx}+k_{dz}2\pi\frac{B}{P}\sin\frac{2\pi}{P}x\right)^2+k_{dy}^2\right]\frac{l^2}{4m}\right\} \quad (E23)$$

The above result is consistent with the result obtained using the incoherent model [Ulaby et al., 1982] where the physical optics solution is averaged over the local slopes. This is due to the fact that when the period P is much larger than the correlation length l, then within the correlation length the periodic component will appear to be planar with the local slope.

Acknowledgments

This work was supported by the NASA Grants NAG5-270 and NAWG-1272, the ARMY Corp of Engineers Contract DACA39-87-K-0022, the NSF Grant 8504381-ECS, and the ONR Contract N00014-83-K-0258.

References

[1] Barrick, D. E., "Relationship between slope probability density function and the physical optics integral in rough surface scattering," *Proc. IEEE,* **56**, 1728–1729, 1968.

[2] Batlivala, P. P. and F. T. Ulaby, "Radar look direction and row crops," *Photogrammetric Eng. Remote Sens.*, **42**, 233–238, 1976.

[3] Beckmann, P. and A. Spizzichino, *The Scattering of Electromagnetic Waves from Rough surfaces*, MacMillan, New York, 1963.

[4] Brown, G. S., "Backscattering from a Gaussian-distributed perfectly conducting rough surface," *IEEE Trans. Ant. Prop.*, **AP-26**, 472–482, 1978.

[5] Chuang, S. L. and J. A. Kong, "Scattering of waves from periodic surfaces," *IEEE Proc.,* **69**, 1132–1144, 1981.

[6] Chuang, S. L. and J. A. Kong, "Wave scattering from a periodic dielectric surface for a general angle of incidence," *Radio Science,* **17**, 545–557, 1982.

[7] Davenport, W. B., Jr. and W. L. Root, *An Introduction to the Theory of Random Signals and Noise,* McGraw-Hill, New York, 1958.

[8] Fenner, R. G., G. F. Pels, and S. C. Reid, "A parametric study of tillage effects on radar backscatter," *Proceedings of the Terrain and Sea Scatter Workshop (TASS),* George Washington Univ., Wash., DC., 1980.

[9] Guissard, A., C. Baufays, and P. Sobieski, "Sea surface description requirements for electromagnetic scattering calculations," *J. Geophys. Res.,* **91**, c2, 2477–2492, 1986.

[10] Hessel, A. and A. A. Oliner, "A New theory of Wood's anomalies on optical gratings," *Applied Optics,* **4**, No. 10, 1275–1297, 1965.

[11] Holzer, J. A. and C. C. Sung, "Scattering of electromagnetic waves from a rough surface II," *J. Appl. Phys.,* **49**, 1002–1011, 1978.

[12] Jordan, A. K. and R. H. Lang, "Electromagnetic scattering patterns from sinusoidal surfaces," *Radio Science,* **14**,1077–1088, 1975.

[13] Kong, J. A., *Electromagnetic Wave Theory,* John Wiley & Sons, New York, 1986.

[14] Leader, J. C., "Bidirectional scattering of electromagnetic waves from rough surfaces," *J. Appl. Phys.,* **42**, 4808–4816, 1971.

[15] Peake, W. H., "Interaction of electromagnetic waves with some natural surfaces," *IEEE Trans. Ant. Prop.,* **AP-7**, Special Supplement, S324–S329, 1959.

[16] Rice, S. O., "Reflection of EM waves by slightly rough surfaces," The Theory of Electromagnetic Waves, M. Kline, Ed., Interscience, NY, 1951.

[17] Sancer, M. I., "Shadow-corrected electromagnetic scattering from a randomly rough surface," *IEEE Trans. Ant. Prop.,* **AP-17**, 577–585, 1969.

[18] Shin, R. T. and J. A. Kong, "Scattering of electromagnetic waves from a randomly perturbed quasiperiodic surface," *J. Appl. Phys.*, **56**, 10–21, 1984.

[19] Stogryn, A., "Electromagnetic scattering from rough finitely conducting surfaces," *Radio Science,* **2**, 415–428, 1967.

[20] Tsang, L. and J. A. Kong, "Energy conservation for reflectivity and transmissivity at a very rough surface," *J. Appl. Phys.*, **51**, 673–680, 1980.

[21] Tsang, L., J. A. Kong, and R. T. Shin, *Theory of Microwave Remote Sensing,* Wiley & Sons, New York, 1985.

[22] Tsang, L. and R. W. Newton, "Microwave emissions from soils with rough surfaces," *J. Geophys. Res.*, **87**, 9017–9024, 1982.

[23] Ulaby, F. T., C. T. Allen, and A. K. Fung, "Method for retrieving the true backscattering coefficient from measurements with a real antenna," IEEE International Geoscience and Remote Sensing Symposium, Munich, **TA-6**, 6.1–6.7, Federal Republic of Germany, 1982.

[24] Ulaby, F. T. and J. E. Bare, "Look direction modulation function of the radar backscattering coefficient of agricultural fields," *Photogrammetric Eng. Remote Sens.*, **45**, 1495–1506, 1979.

[25] Ulaby, F. T., F. Kouyate, A. F. Fung, and A. J. Sieber, "A backscatter model for a randomly perturbed periodic surface," *IEEE Trans. Geosci. Remote Sens.*, **GE-20**, 518–528, 1982.

[26] Valenzuela, G. R., "Depolarization of EM waves by slightly rough surfaces," *IEEE Trans. Ant. Prop.*, **AP-15**, 552–557, 1967.

[27] Valenzeula, G. R., "Scattering of electromagnetic waves from a tilted slightly rough surface," *Radio Science,* **3**, 1057–1064, 1968.

[28] Waterman, P. C., "Scattering by periodic surfaces," *J. Acoust. Soc. Am.*, **57**, 791–802, 1975.

[29] Wright, J. W., "A new model for sea clutter," *IEEE Trans. Ant. Prop.*, **AP-16**, 217–223, 1969.

[30] Wu, S. T. and A. K. Fung, "A noncoherent model for microwave emissions an backscattering from the sea surface," *J. Geophys. Res.*, **77**, 5917–5929, 1972.